



UNIVERSITÀ
DI PAVIA

FACOLTA' DI INGEGNERIA
DIPARTIMENTO DI INGEGNERIA INDUSTRIALE E DELL'INFORMAZIONE
CORSO DI LAUREA MAGISTRALE IN BIOINGEGNERIA

TESI DI LAUREA

TITOLO

G-Force: a high-throughput biomimetic functionalization for drug screening substrates

Candidata: Sara Rigolli

Relatore: Prof. Francesco Pasqualini
Correlatore: Dr. Alessandro Enrico
Controrelatore: Dr. Stefania Marconi

A.A. 2023/2024

TABLE OF CONTENTS

ABSTRACT	4
ESTRATTO.....	6
1. INTRODUCTION	8
1.1 Problem statement and thesis approach.....	8
1.2 Pharmaceutical research process	13
1.3 High-throughput methods for drug screening	15
1.4 Conventional cell culture platforms	18
1.5 Thermodynamics of liquid interface	20
1.6 Surface engineering.....	23
1.6 Gelatin Emulsions	25
1.7 Methods for phase-separation.....	28
2. MATERIALS AND METHODS	31
2.1 Transglutaminase-crosslinked porcine gelatin preparation.....	31
2.2 G-force protocol for thin and flat gels in high-throughput well plates	33
2.3 Image acquisition by confocal microscopy	36
2.4 Image processing and surface analysis.....	36
2.5 Preparation of gelatin substrates for cell culture	38

3. RESULTS	40
3.1 Two-liquid-phase centrifugation approach	40
3.2 Glass activation, emulsion, and centrifugation approach.....	42
3.3 Emulsification is the key step to ensure repeatability	47
3.3.1 Adding a sonication step ensures emulsion stability	47
3.3.2 Is centrifugation necessary?.....	49
3.3.3 Adjusting precursor-in-oil ratio for better control of gelatin height.....	52
4. CONCLUSIONS	57
4.1 Discussion of presented results	57
4.2 Open technical challenges and additional insights.....	59
4.3 Outlook	62
Bibliography	64
Table of figures.....	73
Acknowledgments	78

ABSTRACT

Drug development is becoming increasingly inefficient and expensive, partly due to the poor predictivity of conventional *in vitro* culture models. Traditional preclinical models in which cells grow on plastic or glass lack physiological stiffness and biochemical cues. On the other hand, advanced, biomimetic organ-on-a-chip models are pricey and incompatible with high-throughput screening (HTS). Previous work in the Synthetic Physiology Lab (SPL) at the University of Pavia showed that hydrogel fabrication by automated liquid handling is a viable solution for biomimetic functionalization of high-throughput well plates. Still, surface-energy-driven meniscus formation at the well sidewalls hinders the use of this method for cell culture and microscopy. In particular, a protocol to prepare a cell culture hydrogel with the right thickness (20-200 μm) that covers the entire well of a multiwell plate (0.3-3.5 mm diameter) is missing.

To enable automated fabrication of hydrogels suitable for high-throughput assays, this thesis focused on developing a centrifugation-based protocol, referred to as G-force. With G-force, we can modify the surface free energy of the hydrogel precursor phase cast in high-throughput culture well plates and generate thin flat hydrogels on the whole bottom of the wells. To validate G-force, we performed z-stack fluorescence imaging collecting the signal of fluorescent beads embedded in the hydrogels and we coded a MATLAB routine to extract the hydrogel thickness, roughness, and total 3D volume. In a batch, 40 out of 40 gels resulted in a flat

interface with appropriate coverage and thickness. Further optimizing the hydrogel for optical clarity will provide a biomimetic functionalization to generate a better *in vitro* model and increase the drug screening efficiency in industrial pharmaceutical pipelines.

ESTRATTO

La ricerca farmaceutica sta diventando sempre più inefficiente e costosa, in parte a causa della scarsa predittività dei modelli di coltura *in vitro* convenzionali. I modelli preclinici tradizionali in cui le cellule crescono su plastica o vetro hanno una rigidità non fisiologica e mancano di segnali biochimici. Tuttavia, i modelli biomimetici avanzati come gli organ-on-a-chip sono costosi e incompatibili con i sistemi di *screening* ad alto rendimento. Un lavoro precedente del Synthetic Physiology Lab dell'Università di Pavia ha dimostrato che la fabbricazione di idrogel con sistemi di manipolazione automatica dei liquidi è una soluzione valida per la funzionalizzazione biomimetica delle piastre multipozzetto, ma la formazione di un menisco dovuta al contatto del liquido con le pareti laterali del pozzetto, guidata dall'energia di superficie impedisce l'uso di questo sistema per la coltura cellulare e la microscopia. In particolare, manca un protocollo per la produzione di idrogel per la coltura cellulare del giusto spessore (20-200 μm) che copra l'intero pozzetto di una piastra multipozzetto (0.3-3.5 mm).

Per consentire la fabbricazione automatica di idrogel adatti per saggi ad alto rendimento, questa tesi si è concentrata sullo sviluppo di un protocollo basato sulla centrifugazione, chiamato G-force. Con G-force, possiamo modificare l'energia libera di superficie del precursore dell'idrogel depositato in piastre multipozzetto e generare idrogel piatti sottili sull'intero fondo dei pozzetti. Per validare G-force abbiamo acquisito z-stack in fluorescenza raccogliendo il segnale di biglie

fluorescenti incorporate negli idrogel e abbiamo scritto un codice MATLAB per estrarre lo spessore dell'idrogel, la sua regolarità e il volume 3D totale. In un lotto, 40 gel su 40 hanno prodotto un'interfaccia piana con copertura e spessore adeguati. Un'ulteriore ottimizzazione dell'idrogel per la trasparenza ottica fornirà una funzionalizzazione biomimetica per generare un migliore modello *in vitro* e aumentare l'efficienza dello screening dei farmaci nei processi farmaceutici industriali.

1. INTRODUCTION

1.1 Problem statement and thesis approach

Pharmaceutical industry researchers and operators use the term “Eroom’s law” to describe a puzzling historical trend: the number of approved drugs has remained roughly constant despite an exponential increase in research and development (R&D) investments.¹ The main causes are the duration of the process, which takes about ten years, its cost of over a billion USD, and its success rate of around 10% in the clinical phase.² To counter the loss of efficiency in pharmaceutical R&D, biomimetic *in vitro* models have been proposed with the goal of increasing the quality of the compounds that reach the clinical phase while decreasing the screening costs.³ In fact, drugs undergoing screening are typically tested on 2D cell cultures, that are cell monolayers on a plastic or glass substrate. However, non-physiologically rigid substrates change cell morphology, and consequently their functionality and response to biochemical signals.⁴ These elements decrease the validity of the results from *in vitro* models when extrapolated to human physiology, leading to false-positive preclinical evaluation. In other words, since pharmaceutical R&D has been using poorly predictive pre-clinical assays, it has promoted the wrong compounds to the clinical phases, where 9-out-of-10 of them failed, leading to the paradox described by Eroom’s law.

While different fabrication methods have been proposed to increase the predictivity of *in vitro* models, designing solutions compatible with high-throughput formats and standards is an open technical challenge. Even if depositing a soft and flat layer of relevant biomaterials is simple in low-throughput research settings,⁵⁻⁷ there is a lack of suitable technology for high-throughput functionalization. In fact, using automatic liquid handling to cast a hydrogel solution in a small well typically leads to the formation of a meniscus due to surface tension. When wall-wetting happens the high curvature gel profiles limit the ability to manipulate and optically characterize the models, since cells are on different focal planes and may vary their drug intake, spreading, or gene expression due to the irregular geometry of the underlying substrate. Previous work from SPL addressed the problem by casting and aspirating a small volume of gelatin precursor in the middle of the well, without touching the sidewalls. However, this approach needs careful calibration to avoid wall-wetting, which is hardly scalable to 1534-well plate formats, and the hydrogel functionalization covers only part of the well substrates (~ 40% of coverage).

To fill the gap between high-cost but highly biomimetic 3D cultures and traditional cell monolayers on stiff substrates, in this thesis, we propose to exploit liquid handling robots, a technology already present in pharmaceutical pipelines, to functionalize the multiwell plates with a complete coverage thin hydrogel layer. The aim of our work is to develop a protocol to produce a simple and cost-effective platform suitable for high-resolution microscopy and omics assays on cells,

growing them on a soft, flat, and homogeneous substrate. We aim to develop a reproducible pipeline for gelatin-based hydrogel production and analysis, relying on a two-liquid-phases and centrifugation approach to counterbalance thermodynamic forces and avoid meniscus formation. In particular, we need to compensate for the imbalance between surface forces, i.e. pressure and interfacial tension, and volume forces, i.e. gravity, and for the capillary rise along walls due to the delta in the interfacial tension between a liquid-solid and an air-solid interface.^{8,9}

To offset the surface forces, a simple approach is to increase gravity by centrifugation. However, capillarity is still a crucial phenomenon in high-throughput well plates due to the geometry of the wells, and centrifugation alone is not sufficient to obtain a completely flat interface. To neutralize the capillary rise, it is necessary to square the interfacial tension between the gelatin precursor and the other fluid in contact with the sidewalls of the multiwell plate. Our idea is to create a two-liquid-phase interface, using a second liquid that is lighter than and immiscible with gelatin precursor, or rather with water that is the hydrogel main component. Other requirements for the second phase are compatibility with cell growth, and having a similar contact angle, a measure of interfacial properties, with sidewalls.^{8,9} If the interfacial tension between the solid and each liquid is the same, there is no reason to have a capillary rise at the sidewalls, so we should obtain a flat interface between the gelatin and the second phase and a meniscus between it and air as illustrated in **Figure 1**. For a cost-effective solution, we

propose vegetal oils, in particular sunflower seed oil, as the second liquid. Vegetal oils meet the requirement of immiscibility and density, moreover, they are non-toxic and have a viscosity compatible with liquid handling robots.

To flatten the interface, however, surface engineering the interfacial forces is not sufficient, and we need to compensate also for the imbalance of volume and surface forces, which are prevalent in a microfluidic environment. To this end, we suggest centrifugation to increase the gravity to which the plate is subjected up to 4000g as a technique to counterbalance the surface forces. Moreover, centrifugation guarantees phase separation at the interface, favoring the oil removal for cell growth. Yet, to obtain complete spreading and a flat interface we need to combine emulsification with centrifugation, breaking the continuity of gelatin which otherwise tends to stick together and to form rounded profiles.

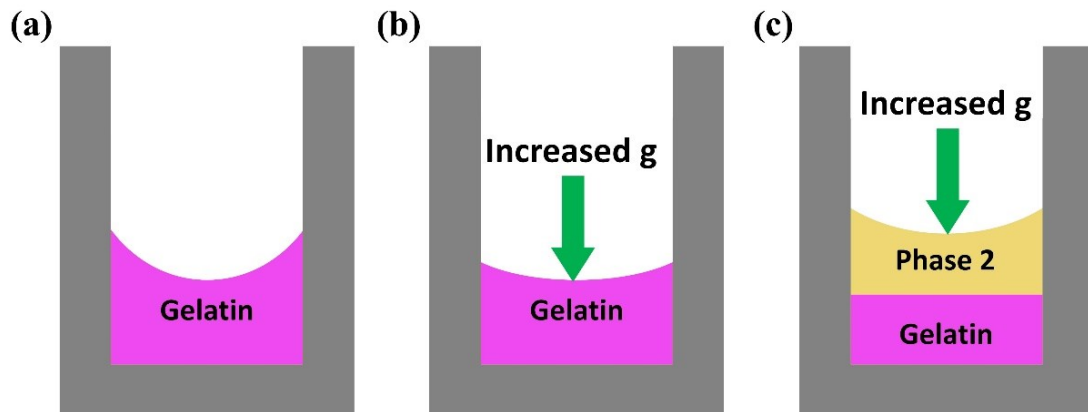


Figure 1 Schematic idea of the work. (a) is a schematic of the profile of an interface with a meniscus. (b) is a schematic of the flattening due to the increase in gravity. (c) is a schematic of the profile when a second liquid phase and an increase in gravity are combined as in G-force.

However, for our goals identifying good candidates for the second phase is just the first step. We also need to fix the requirements to deem our experiments successful with respect to the aim to produce platforms compatible both with microscopy and

omics. To ensure that our pipeline is compatible with high-resolution microscopy, we develop the protocol on glass-bottom well plates. We fix 200 μm as the upper limit of the permissible gel height range to ensure that the hydrogel top is within the working distance of a 100x objective (typically around 350-400 μm). We set the lower limit to 20 μm to ensure that cells sense only the mechanical stimuli from the soft hydrogel being isolated from the stiff substrate.¹⁰

Furthermore, to meet the omics requirements for a single population of cells that sense the same mechanical stimuli, we only deem acceptable the gels with a calculated bottom coverage greater than 80%, accounting for underestimation errors due to pixel-to-micron conversions. To enhance the spreading of the gelatin layer on the whole well, we implement a NaOH treatment, which decreases the contact angle of the glass substrate by exposing negative charges, favoring the adhesion of gelatin.¹¹ Lastly, we develop an image analysis and surface reconstruction routine coded in MATLAB to extract the characteristic parameters of the produced gels and discuss the experimental results.

1.2 Pharmaceutical research process

The pharmaceutical research pipeline is strictly codified to ensure that the drugs approved are effective and their side effects are minimized. However, this process is inherently inefficient as it requires over 10 years and investments of over 1 billion dollars for a failure rate of up to 90%.² A schematic of the pipeline is shown in **Figure 2**. At first, libraries of chemical compounds are screened to identify possible molecular mechanisms that can intervene against a disease. The most promising compounds are then subjected to preclinical testing. In this phase, potential drugs are tested on *in vitro* models to verify cytotoxicity and efficacy on cell populations.¹² Drugs that show promising results and do not do significant harm to cell cultures progress to testing on *in vivo* animal models, however, the scientific community aims to develop tools to remove this step from drug discovery pipelines. If a compound shows efficacy and non-toxicity during the preclinical *in vivo* testing, it progresses to the clinical trial.¹² The clinical trial is the longest and most expensive phase of the process, which accounts for 50-60% of the total costs of drug discovery and is successful only in 1 out of 10 cases.²

To reduce the costs of pharmaceutical research, reliable *in vitro* models are fundamental, as failing in this phase is cheaper than in the clinical phase. Moreover, biomimetic *in vitro* models could better recapitulate human physiology, overcoming the need for animal testing. However, to effectively impact the costs, innovative *in vitro* models should be produced from cheap materials and provide

platforms that can be easily integrated with standard testing, such as HTS techniques.

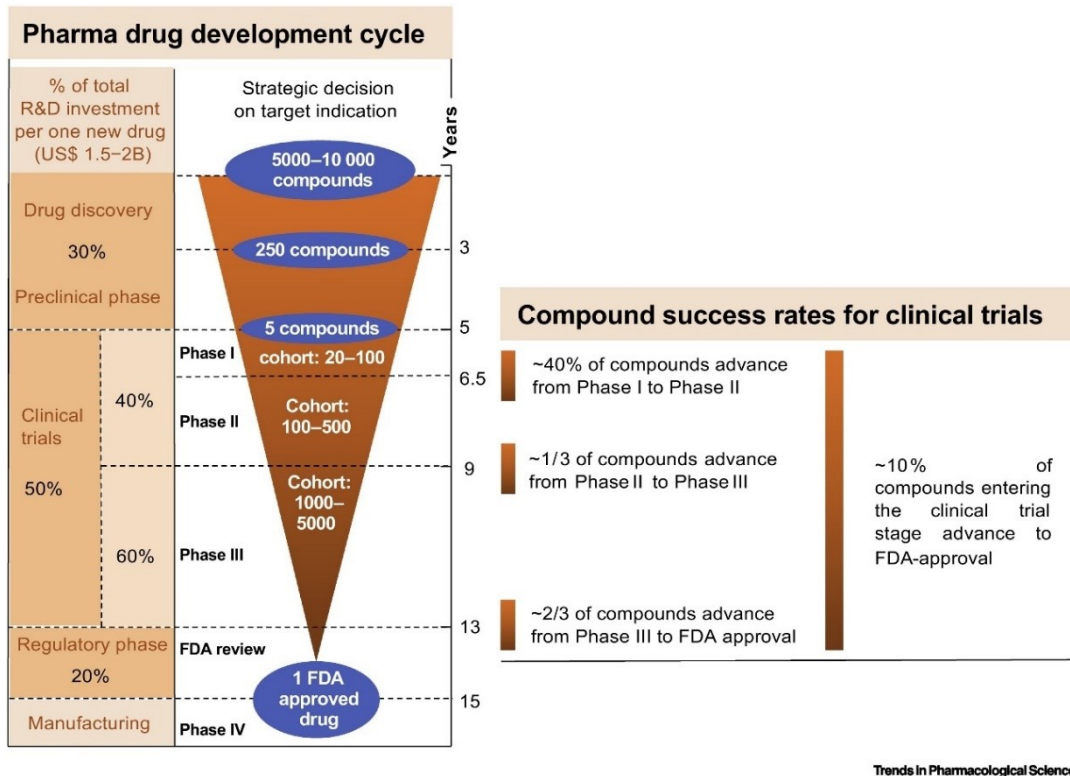


Figure 2 Description of drug development pipeline phases, times, and costs. Reproduced from².

1.3 High-throughput methods for drug screening

During the preclinical stage of pharmaceutical research, hundreds of different compounds are screened. To minimize the resources needed to assess drug toxicity and efficacy, both laboratory settings¹³ and pharmaceutical R&D¹⁴ adopted high-throughput assay methods. These methods permit a rapid and parallel assessment of the variation of target parameters in multiwell plates where cells are treated with different compounds, doses, or administration protocols.

One of the most flexible methods for HTS is microscopy, as a variety of relevant parameters to describe cell response to drugs can be extracted from images. In particular, pharmaceutical research relies on changes in the cell phenotype¹⁵ and quantification of fluorescent signal associated with specific proteins¹⁶ in large and automatically analyzed datasets to determine if statistical differences arise between groups of cells subjected to different treatments.¹⁷ A schematic of the HTS process by microscopy imaging is shown in **Figure 3a**.

Even if microscopy is the most common data source in HTS, other assays have historically been relevant in pharmaceutical research. In particular, genomics, metabolomics, transcriptomics, and other “omics” analyses are significant in compound screening^{18,19} as they can reduce the need for animal testing, bridging the gap between *in vitro* and *in vivo* models.²⁰ These assays are based on extracting and quantifying genetic material or transcripts in cells and comparing the values

between populations to verify if and how drugs interact with the genome expression.

The culture substrate chosen for cell growth plays a crucial role in the reliability of omics assays and, therefore, is a factor that greatly affects the compatibility of the designed platform with current pharmaceutical screening pipelines. The method previously developed in SPL for biofunctionalization suffers from limited well-bottom coverage. Seeding cells in such functionalized wells results in two cell populations depending on whether they are adhering to the soft hydrogel or the stiff well bottom, as shown in **Figure 3c-d**. However, to lead to meaningful results, omics must be performed on a single population of cells, meaning that cells should receive the same biochemical and mechanical cues. Running meaningful omics assays on mixed cell populations would require the ability to select the source of the analyte. While single-cell²¹ and spatial-omics^{22,23} approaches are available, they are not economically viable solutions for HTS, where bulk extraction of molecular constituents (DNA, RNA, protein, ...) remains the only possible option. The association between assays and material extracted from cells is described in **Figure 3b**.

From a practical standpoint, these considerations lead us to desire HTS platforms where all the cells on a given well are grown on a material with native-like chemo-mechanical properties. For example, we might want a substrate with the stiffness of soft biological tissues, ~10 kPa. But, today, cells are grown on 100x-100,000x stiffer substrates.

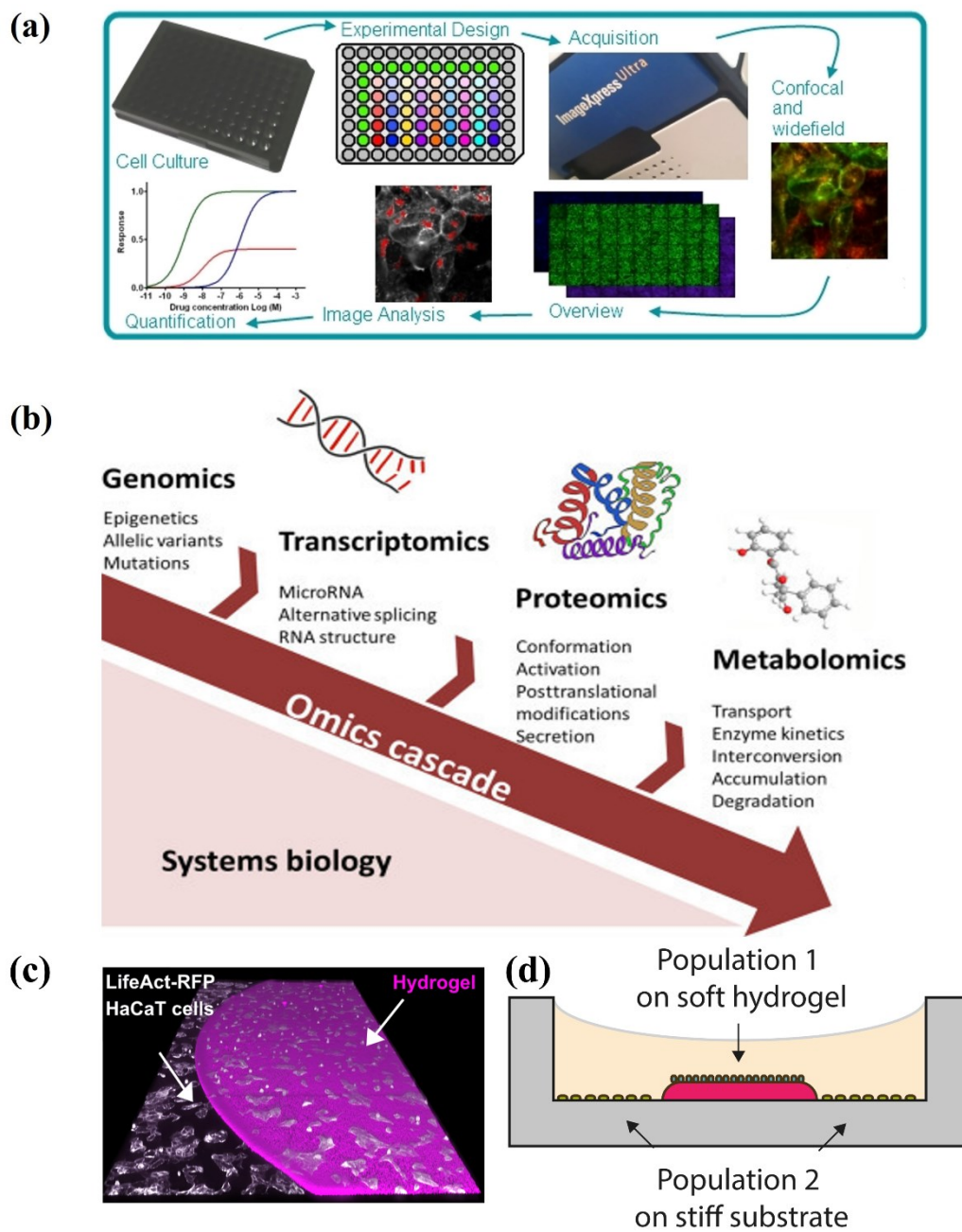


Figure 3 Schematics of main high-throughput screening methods. (a) Schematics of microscopy screening pipeline. Reproduced from²⁴. (b) Description of the targets of “omics” assays. Reproduced from²⁵. (c) 3D rendering of HaCaT cells (human keratinocytes, in white) seeded on gelatin hydrogel with fluorescent beads (in magenta). Reproduced from previous SPL work. (d) Schematics representation of (c) displaying the mixed cell populations, which is a problem for omics assays.

1.4 Conventional cell culture platforms

Drug screening heavily relies on cell culture in the early stage of preclinical research,²⁶ in particular, to test the cytotoxicity of compounds.²⁰ However, traditional cell culture platforms fail to be predictive *in vivo* models, and existing predictive ones, like organs-on-chips, are not compatible with HTS (**Figure 4**).²⁷ To meet the high-throughput requirements, pharmaceutical research relies on traditional 2D monolayers grown on stiff material, such as glass or plastic. Yet, these platforms fail to provide relevant physiological stimuli, such as chemical signals or matrix-cell interactions. Moreover, the mechanical response to hard substrates causes changes in the cell structure and phenotype, affecting drug intake and gene expression. These factors combined make traditional culture substrates poor *in vitro* models and contribute to late-stage drug testing failure.^{4,20,27}

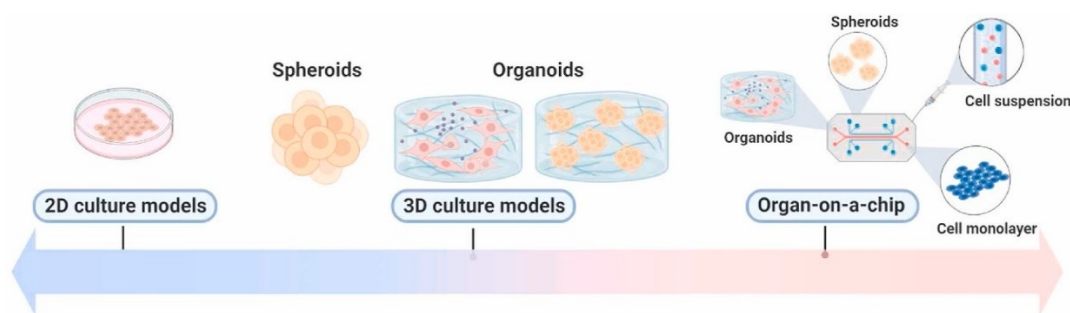


Figure 4 Existing cell culture platforms. From left to right the microenvironment becomes more biomimetic, but also more expensive. Figure reproduced from²⁸.

Different 3D platforms are proposed to overcome these challenges, such as spheroids, organoids, and organs-on-chip. These structures can better mimic *in vivo* architectures and mechanical stimuli and are viable for the co-culture of different relevant cell populations.²⁹ Although new protocols are working to make

spheroids and organoids compatible with HTS pipelines³⁰ due to their complex 3D structure, they are not easily compatible with high-throughput microscopy or functionality assays,³¹ and standard HTS assays based on chromophores or fluorophores can produce false results.³² Moreover, spheroids and organoids grown in suspension only recapitulate cell-cell interactions, lacking extracellular microenvironmental cues. However, embedding cultures in hydrogels is a viable solution to recapitulate extracellular cues and integrate nutrition and oxygen intake by diffusion.³³ These platforms, although, are pricey, poorly compatible with microscopy due to the porosity-enhanced scattering,³⁴ and hardly predictive of dosages because embedded cells are less sensitive to potential treatment.³³ Organ-on-chip are engineered substrates that can effectively recapitulate the structure, stiffness, mechanical stimuli, and fine microenvironmental properties of the organ or tissue of interest, however, they are viable only for small-scale production and not optimized for HTS pipelines.³¹

1.5 Thermodynamics of liquid interface

To overcome the high costs and long times to develop safe and effective drugs, pharmaceutical research needs new and more reliable platforms to test compounds in the early preclinical stage.³ The Synthetic Physiology group at the University of Pavia focused on coating the traditional stiff substrate with a thin layer of relevant biomaterials, i.e. gelatin-based hydrogels, to improve the efficiency of drug screening maintaining a simple and cost-effective approach. However, casting a hydrogel solution in a small well causes the rise of a meniscus at the air-liquid interface: due to its significative curvature, the platform is no longer suitable for microscopy and “omics” assays due to the presence of cells on different focal planes, which are also subjected to various mechanical stimuli. To overcome this challenge, we investigated the phenomena underlying the meniscus formation to develop strategies to overcome its physical causes. On the microscale of HTS plates, surface forces, such as surface tension and capillarity, dominate volume forces, in particular gravity.³⁵

Classically, the meniscus rise is described as a capillarity phenomenon driven by the difference in interfacial tension in a fluid/fluid system meeting a solid wall.⁸ To eliminate the driving force, we need a reliable quantification of the interfacial tension between two fluids, such as gelatin precursor and air or gelatin precursor and another liquid. Yet, obtaining this measure is not trivial, due to the technical complexity of the proposed protocols, which include pendant drop tensiometry,³⁶ drop weight method,³⁷ and the ring-pull method.³⁸ However, in a thermodynamic

approach, the driving force is the free surface energy difference between the solid-fluid 1 (gelatin) interface and the solid-fluid 2 (air or second liquid) interface.⁹ The relationship between the free surface energy difference ($\Delta\gamma^s$) and the interfacial tension between the two fluids (γ) is described by the following equation: $\Delta\gamma^s = \gamma \cos(\theta)$, where θ is the contact angle between the two fluids, that describes the curvature angle at the solid boundary as shown in **Figure 5**.

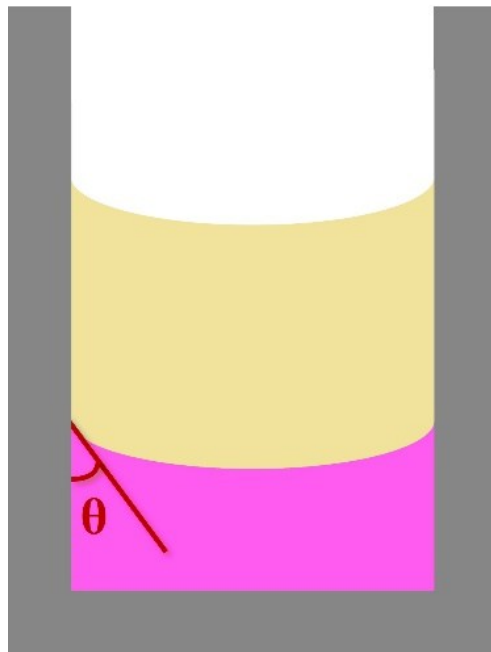


Figure 5 Schematics of the contact angle at a two-fluid interface with a solid well. Bottom liquid (magenta) represents the biomaterial precursor, with on top the immiscible liquid (yellow) added as the second phase. At the interface between the two and the solid interface the contact angle is highlighted. The interface between these two liquids is the surface on which the cells will grow once the biomaterial will harden and the second liquid will be removed.

Since the goal is to obtain a flat interface, we can describe this aim as having $\theta = 90^\circ$, which results in $\Delta\gamma^s = 0$. That demonstrates that adding a second liquid with the same surface energy as our hydrogel precursor is a theoretical solution to flatten the interface. Focusing on liquids immiscible in water, which is the main

component of our hydrogel precursor, and looking for a liquid less dense than water and non-toxic for cell growth, we focused on vegetal oils. In particular, we selected food-grade sunflower seed oil as a readily available, cost-effective, and high-surface energy candidate for our experiments.

However, finding a suitable liquid is just one of the requirements, because two other factors intervene in our experiments. First, the equations above rely on the assumption that there is no interface between the second lighter liquid and the bottom surface. To ensure that this assumption holds, we need to modify the bottom surface of the well. The other assumption is that the contact angles between each liquid and the solid are constant, yet gelatin precursor wetting the sidewalls modifies their contact angle, favoring gel adhesion that is also enhanced due to the tendency of gelatin to stick together. Thus, we propose to reduce this problem by breaking the continuity of gelatin, using the technique of emulsification.

1.6 Surface engineering

To achieve complete coverage of the well bottom surface, we propose to engineer its physical properties to increase the precursor spreading by lowering the contact angle. Common methods for lowering the contact angle of glass are plasma treatment,³⁹ and chemical treatment with acids or bases (**Figure 6**).^{11,40}

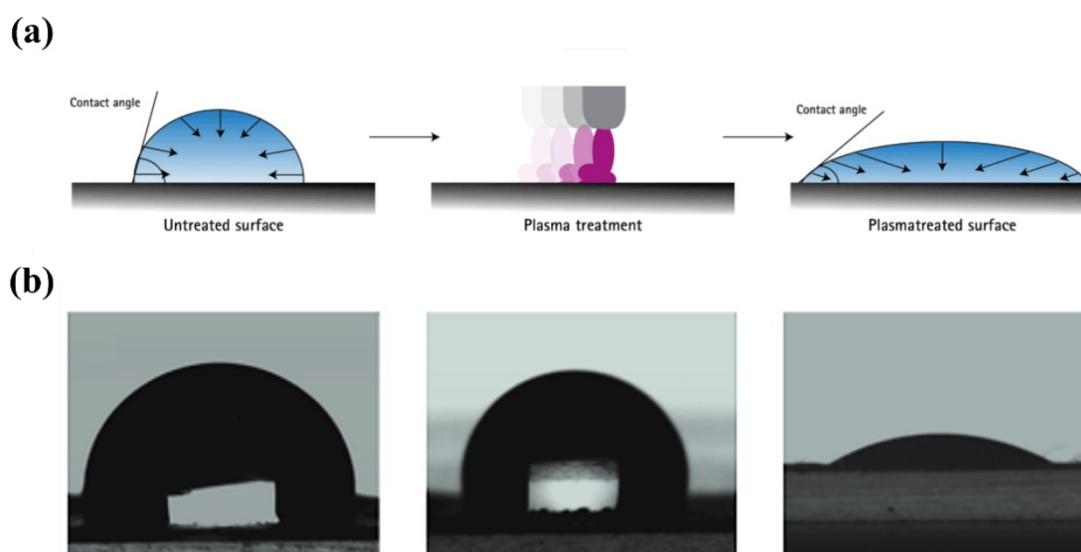


Figure 6 Changes in contact angle before and after surface treatment. (a) Schematics of contact angle changes after plasma treatment. Adapted from ⁴¹. (b) Changes in contact angle after chemical NaOH treatment: untreated substrate, 0.1M treated substrate, 1M treated substrate. Adapted from ⁴²

While plasma treatments on different materials typically lead to a similar decrease in contact angle, chemical treatments produce different wetting properties depending on the treated material. Therefore, having a glass bottom substrate and polystyrene sidewalls makes chemical functionalization ideal for selectively increasing the wetting of the bottom substrate. In particular, we used NaOH to decrease the contact angle of the glass substrate. In fact, NaOH activation decreases the contact angle between glass and water to values below 25° ,¹¹ and can

be effectively removed by rinsing three times the substrate with DI water.⁴³ To ensure that activation is effective, we performed experiments on the multiwell plates within 30 minutes after the activation.

1.6 Gelatin Emulsions

To counterbalance the tendency of gelatin to stick together and functionalize the substrates to favor further adhesion, we need to break its continuity with an emulsion. To form an emulsion, it is necessary to disperse a liquid in an immiscible liquid.⁴⁴ Typically, emulsions are composed of a continuous phase and a dispersed phase in the form of droplets.⁴⁴ Common examples of liquids that form emulsions are water and oil. They can combine in different forms: water-in-oil emulsions, where oil is the continuous phase in which water is dispersed, oil-in-water, where the opposite happens, and more complex geometries, like water-in-oil-in-water or oil-in-water-in-oil, where two orders of droplets are formed inside one another (Figure 7).

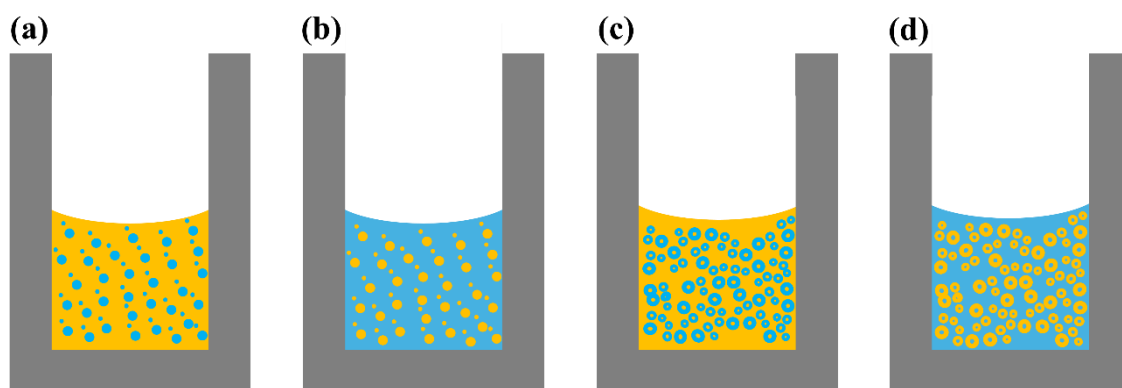


Figure 7 Different kinds of emulsions of water (blue) and oil (yellow) in a well. (a) water-in-oil, (b) oil-in-water, (c) oil-in-water-in-oil, (d) water-in-oil-in-water.

However, two immiscible liquids are necessary but not sufficient to form an emulsion. In fact, the presence of immiscible liquids is just one of the three criteria needed to obtain an emulsion, the other two are an emulsifying agent and availability of mixing energy.⁴⁵ An emulsifying agent is a molecule characterized

by both hydrophilic and hydrophobic residues that can interact at the interface of the liquid phases to stabilize the emulsion. In the absence of an emulsifier, the surface interactions cause the droplets to coalesce, meaning that the droplets rapidly merge again, segregating the emulsion into two separated continuous phases, the mechanisms of separation are shown in **Figure 8**. Due to its amphiphilic nature, determined by the presence of both hydrophilic and hydrophobic residues in the chain, gelatin is a natural emulsifier largely diffused in the food industry.⁴⁶ Thus, our hydrogel precursor includes naturally both the aqueous phase and the emulsifier. Moreover, the presence of the crosslinker mTG contributes to further increasing the emulsion's stability.⁴⁷

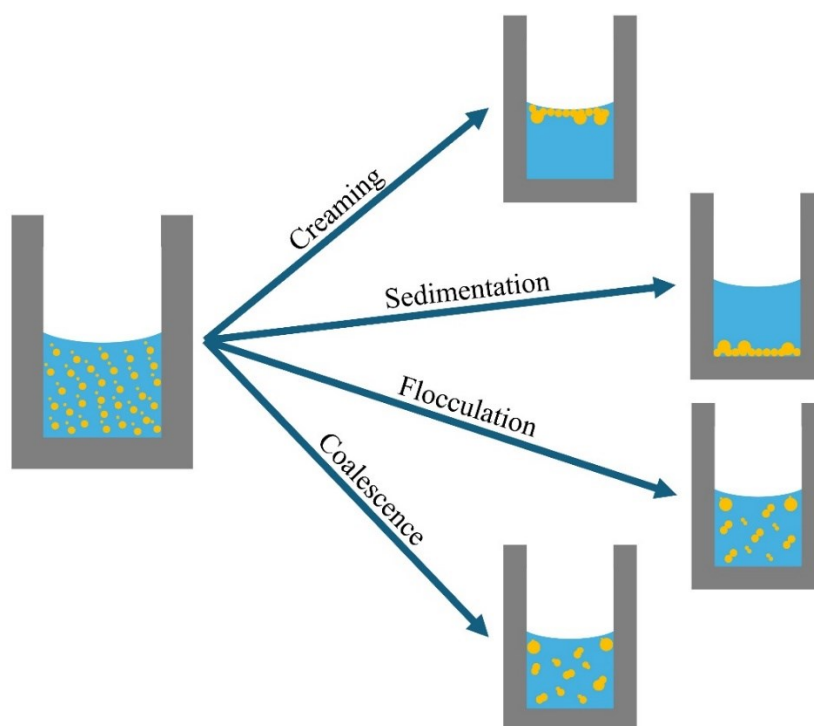


Figure 8 Mechanisms of emulsion separation. Creaming happens when the lighter phase rises to the surface, while sedimentation occurs when the denser phase precipitates at the bottom. Flocculation occurs when the droplets form a larger cluster without merging, while coalescence happens when droplets aggregate by merging.

The most common emulsion mixing methods compatible with a laboratory setting are microfluidization,⁴⁸ sonication,⁴⁹ and stirring.⁵⁰ Microfluidization relies on pumping the two phases in two microfluidic channels that converge, making the flows collide at high pressure. Inertial forces, turbulent flow, and cavitation determine the disruption of one liquid into droplets.⁴⁸ Microfluidization produces fine emulsions of droplets with a narrow range of diameter. However, due to the nature of the technique, viscous liquids can be challenging, requiring high pumping energy to mix. Sonication produces high-energy acoustic waves that transfer mechanical energy to the system after traveling in a bath where a container with the two phases is submerged. Sonication provides significant amounts of energy to the liquids, forming emulsions with high stability. However, the droplet diameter range is wider than in emulsions produced with microfluidics systems.

Stirring exploits an analogous physical principle as it transfers mechanical energy to liquids. However, this method involves longer mixing times to obtain stability, and results depend on other factors, such as mixing velocity and temperature.⁵⁰ Since we need the mixture to remain stable during the casting process to ensure repeatability in the amount of gelatin cast in each well, we plan to use sonication to form the emulsions. In fact, the equipment for microfluidization was not available, and stirring had an expected longer manufacturing time and a complex relationship with heating⁵⁰ that we ignored at the moment.

1.7 Methods for phase-separation

After producing and automatically casting the emulsion, we need to separate the hydrogel precursor from the sunflower seed oil in two continuous phases again to exploit the two-liquid approach's advantages in flattening the interface. Theoretically, phase separation occurs spontaneously in a two-phase system of immiscible liquids due to coalescence and sedimentation. However, as illustrated in the previous section, we have to increase the emulsion stability to obtain an even distribution of gelatin precursor in oil, inhibiting spontaneous phase separation.

Yet, to obtain a flat and optically transparent layer of gelatin-based hydrogel on the bottom of our wells, we need to induce phase separation while the gelatin is setting, to exploit the introduction of the second liquid to flatten the interface. Moreover, emulsion droplets trapped in the gelatin chains introduce scattering factors, reducing the microscopy imaging resolution. Furthermore, growing cells on platforms containing vegetal oil can lead to false results in drug response tests if the oil is slowly released in time, and the droplets can also produce different mechanical stimuli along the gelatin layer with consequences on cells.

The state-of-the-art technique to enhance phase separation of stable emulsions of oil and water is centrifugation.^{51,52} Centrifugation determines phase separation based on density due to the effect of increased gravity on different liquids: the denser tends to sink while the lighter tends to move in the opposite direction of centrifugal force.⁵³ Centrifugation is particularly appealing for our application

because of its two purposes: while inducing phase separation, it also opposes the capillary rise by counterbalancing surface and volume forces due to the increase in gravity, as shown in **Figure 9a**. However, due to its amphiphilic nature, gelatin is a surfactant that increases the emulsion stability, particularly in hydrogel precursor solutions containing a moderate amount of mTG.⁴⁷ If the emulsion is so stable that centrifugation alone is insufficient to induce phase separation, other factors can intervene, such as chemical modification. Chemical compounds called “demulsifiers” have been used since the 1920s as they are adsorbed at the water-oil interface modifying interfacial properties to induce coalescence.⁵²

A different approach is exploiting the protein content of gelatin to induce its precipitation. To achieve this result, two commonly used techniques are salting out and chemical precipitation,⁵⁴ shown in **Figure 9b-c**. One of the most common methods for chemical demulsification is adding ethanol to the mixture. Ethanol decreases the solubility of amino acids inducing the separation of solutes from solvents, acting as a demulsifier.⁵⁵ However, high concentrations of ethanol denature the proteins unfolding the gelatin chains with negative consequences on the biocompatibility and signaling between the substrate and the cells.⁵⁶ The salting out technique is based on the Hofmeister effect, which was first described in 1888 as the capacity of different salts to induce a decrease or an increase of the water solubility of nonelectrolytes, referred to as “salting out” and “salting in”.⁵⁷ Salting out is caused by the dissolution of small anions in the aqueous phase, anions repel solutes determining their precipitation.⁵⁸ This principle is very

effective in separating organic solutes from liquid solvents, however, several studies demonstrate that the thermal, mechanical, and structural properties of gelatin are severely modified during the process.^{54,59} For these reasons, we proposed centrifugation as the preferred method for phase separation

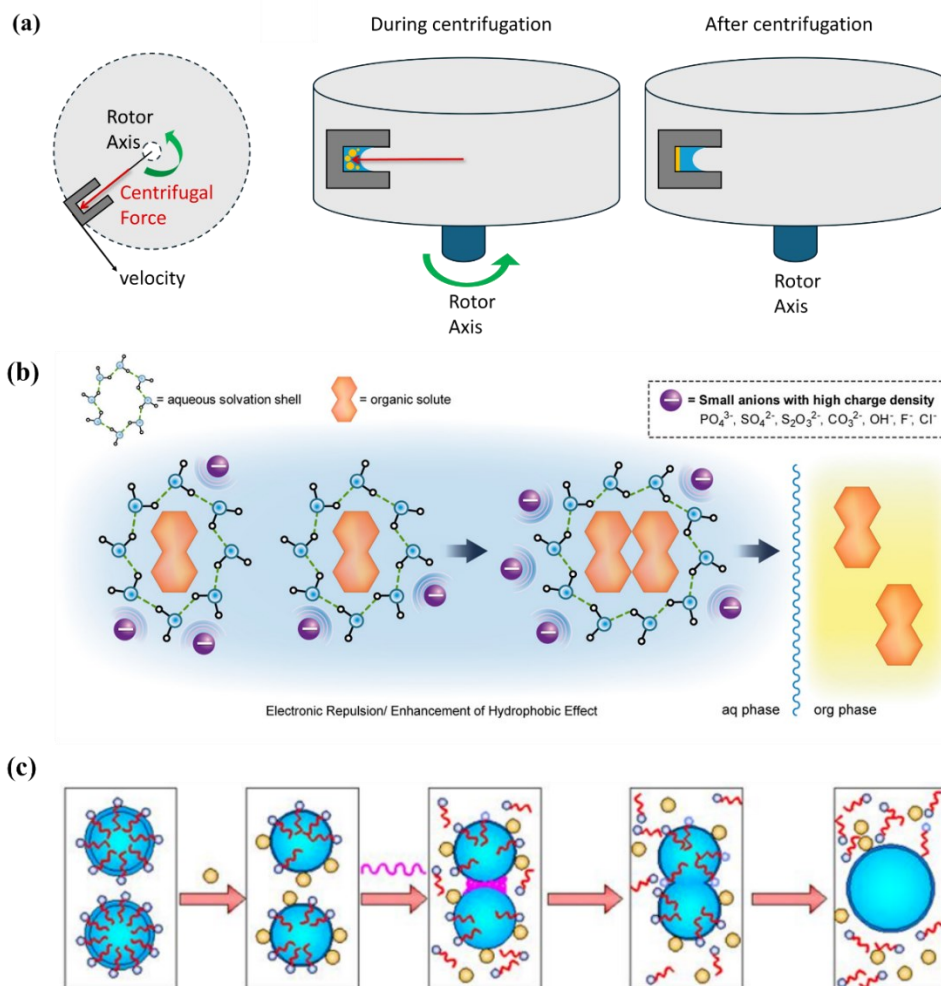


Figure 9 Phase separation methods. (a) Schematics of centrifugation process. Due to the increase in gravity (i.e centrifugal force) the denser liquid (in yellow), is subjected to higher force during centrifugation and precipitate at the bottom of the well. (b) Schematics of salting out process due to increase in ion concentration. Reproduced from⁵⁸. (c) Schematics of chemical demulsification. When a demulsifier (yellow dot) is added to the emulsion it competes with the surfactant at the drop interface. Due to its specific properties, the repulsion between drops lessens and coalescence occurs, the drops merge and become denser allowing phase separation. Reproduced from⁶⁰.

2. MATERIALS AND METHODS

This section describes the procedures we followed to prepare the hydrogel precursor solution. Then, the protocol we implemented to obtain a hydrogel layer in high-throughput well plates is reported in detail. Furthermore, the microscopy setup for image acquisition is presented. Moreover, the MATLAB script for image analysis and gel surface and profile reconstruction is briefly illustrated. Besides, the procedure to make the gels suitable for cell growth is explained. Lastly, another technique to tune the gel height due to differences in osmolarity is discussed.

2.1 Transglutaminase-crosslinked porcine gelatin preparation

To generate a physiologically relevant environment for cell growth, we used a gelatin-based hydrogel precursor needed to coat the bottom of multiwell plates. Stock solutions of 10% w/v porcine gelatin (PG) and 2% w/v microbial transglutaminase (mTG) were prepared under a biological hood to avoid bacterial contamination, stored at 4°C in sealed tubes, and used within a week.

To get a 10% w/v gelatin stock, 500 mg of gelatin from porcine skin (Sigma, G2625-500G) were dissolved into 5 mL of Dulbecco's phosphate buffered saline (PBS) without Ca²⁺ and Mg²⁺ (referred to as "PBS -/," C-40232, PromoCell).

To facilitate the dissolution of the powdered gelatin, PBS -/- was placed in a beaker with a magnetic stirrer, and the beaker was put on a magnetic hotplate. The solution was heated at 70°C and magnetically stirred at 1300-1500 rpm while adding gradually the gelatin powder. The solution was mixed for about an hour until it was clear.

PG physically crosslinks at room temperature forming a triple helix network by hydrogen bonds and hydrophobic interactions⁶¹, however, due to the weak nature of these bonds, the network has poor physical properties and is easily dissociated or degraded by a change in the external conditions⁶². To guarantee the stability of the gelatin networks in long-term experiments or storage, a chemical cross-linker capable of forming stable covalent bonds is required. To this end, we used mTG as a state-of-the-art enzyme in the food and pharmaceutical industries to obtain a stable, three-dimensional, covalently cross-linked network of proteins or polymers containing glutamine and lysine groups^{63,64}.

To prepare the 2% w/v mTG stock solution, 100 mg of mTG (Activa® TI Transglutaminase, product number 1002, Modernist Pantry) was dissolved in 5 mL of PBS -/- by magnetic stirring at 1000 rpm for at least 10 minutes at room temperature. The solution was filtered through a 0.45 µm filter and placed in sealed tubes to be stored at 4°C until use.

2.2 G-force protocol for thin and flat gels in high-throughput well plates

To avoid the natural formation of optically challenging curved hydrogels in high-throughput well plates due to surface tension, we developed a protocol that combines the emulsification of gelatin precursor solution in an immiscible liquid, such as oil, and the centrifugation of the plate containing the mixture.

First, we treated the bottom of the plate to decrease the water contact angle. To this end, the bottom of the wells of a 384-glass bottom well plate (Cellvis P384-1.5H-N) was activated by soaking with 1M NaOH. 10 μ L of NaOH were cast in each well and spread by putting the plate in the centrifuge (Thermo Scientific™ SL 16 Centrifuge 75004031) to give it an impulse until reaching 1000 g. Then, the plate was left under the biological hood for about 1h to complete the activation process. Finally, the wells were washed three times with sterile deionized water (DI water) by casting 80 μ L of DI water in each well and aspirating the liquid with a vacuum system. The plate was left open under biohood for at least 15 minutes to ensure complete drying.

Then, we mixed the gel precursor with sunflower seed oil. Specifically, the PG and mTG stock solutions were heated at 37°C in the hot bath for at least 30 minutes to ensure the best working conditions. A food-grade vegetal oil (commercial sunflower seed oil purchased at a local store) was filtered through a 0.22 μ m filter under the biological hood to ensure sterility and placed in a sealed tube. Then, it

was also placed in the hot bath until it reached 37°C. When the liquid components were warm, they were mixed in a 1:1 oil-to-precursor ratio following the subsequent steps. First, a fixed quantity of mTG was placed in an Eppendorf tube, i.e. 250 μ L to obtain a final mixture volume of 1 mL. To ensure a good optical signal for microscopy gel characterization, the FluoSpheres™ carboxylate-modified, 0.2 μ m, dark red (660/680) (Thermo Fisher Scientific, F8807) was added to the mTG in a 1:100 beads-to-precursor volume ratio (5 μ L of beads in 250 μ L of mTG).

The liquid mixture was then vortexed and sonicated to produce an emulsion. To avoid the formation of clusters of beads, the mTG aliquot containing beads was sonicated for 5 minutes. Then, the same amount of PG, i.e. 250 μ L in this example, was added in the Eppendorf, and mixed by pipetting until a clear appearance was reached. After that, a double volume of sunflower seed oil, i.e. 500 μ L, was put in the Eppendorf vial and pipetted again. To form an evenly distributed emulsion, the vial was vortexed for 10 seconds, sonicated for 10 minutes in warm water to prevent an early setting of hydrogel, vortexed again for 10 seconds, and then used within 15 minutes.

The emulsifier mixture was cast in 384 well plates, and the plates were centrifuged to facilitate creaming and sedimentation of the hydrogel into a flat thin layer at the bottom of the well. The vial contained a white foam that was poured into a reservoir and cast in the well plate with a liquid-handling robot. To obtain thin gels suitable for microscopy, in each well a volume of 4 μ L was cast at low speed to

control the volume due to the viscosity of the emulsion. Finally, the plate was rapidly transferred to the centrifuge precooled at 4°C to obtain phase separation between the oil and the gelatin precursor. To get a flat interface, gravity must be increased to overcome surface forces that would otherwise form a meniscus and to break the emulsion. Specifically, the centrifugation was run to have the plate experience 4000g. Moreover, to ensure that both physical and enzymatical crosslinking were initialized, the time of rotation was fixed at 20 minutes.

2.3 Image acquisition by confocal microscopy

To determine if the coating layer matched the goal parameters for high-resolution microscopy, the gels were characterized by confocal imaging. Images were acquired using a Nikon Eclipse Ti2 inverted microscope featuring a Crest V3 X-Light spinning disk confocal, Lumencore Celesta Light Engine source for the 638 nm radiation, and a Photometrics Kinetix Scientific CMOS camera. To excite the fluorescent beads embedded in the hydrogels, an exposure time was set between 5 to 15 ms. All images were acquired in confocal microscope mode using a 20X air objective (N.A. 0.75, product number MRD00205, Nikon), and acquiring multiple planes with a step of 0.9 μm in between to ensure high resolution. The z-stack was acquired from an out-of-focus plane without signal, whose acquisition was later used to remove the plate autofluorescence noise, to the automatic perfect focus height. Images were acquired in large image mode, and the final field of view covered a (3.5 x 3.5) mm^2 area containing the whole well, the final image was given by the juxtaposition of 16 tiles blended with a 5% overlap. The image had an 8-bit depth and 4x4 binning was performed to enhance the signal-to-noise ratio and reduce the file dimension.

2.4 Image processing and surface analysis

To demonstrate that the layer cast in the wells matched the goals set for high-resolution microscopy and drug screening, the following image analysis routine

was implemented. First, the images were uploaded to the ImageJ Fiji software where a gamma correction factor of 1.4 was applied to the stack to increase the signal-to-noise ratio. This value was selected sweeping on a range of positive gamma factors, as it is the minimum value that removes single-pixel signal artifacts, as the dimension of beads is larger than a single pixel. Furthermore, the out-of-focus frame acquired as the start plane of the z-stack, selected as the automatic-detected air-glass interface at the bottom of the plate, was subtracted from each frame to remove the autofluorescence noise. Finally, the histogram was automatically adjusted, and the corrected image was saved in TIFF format.

After that manual procedure, an automatic MATLAB routine was performed. This routine is coded to iterate on all TIFF files in a user-selected directory and for each image it extracts the mean height of the gel as the number of planes in which a signal is detected over an automatically defined threshold with Otsu's method multiplied for the in-between-planes step of $0.9\ \mu\text{m}$, and it calculates the standard deviation of height as a measure of the gel flatness and surface roughness. From the mean height of the gel, the volume of precursor solution cast in each well is inferred by converting in microns the area of the detected signal in each plane and multiplying the value for the step factor of $0.9\ \mu\text{m}$. The volume of each plane is then added to extract the total volume. Lastly, an underestimation of the percentage of the well coverage is extracted from the z-max projection of the image. We set 80% of estimated coverage as the lower percentage that ensures complete coverage due to several factors of underestimation, such as the approximation during pixel-

to-micron conversion, the cuts in the image due to a misalignment of the CMOS camera, and air bubbles inclusion that scatter the signal of the upper gel layer that is consequently deemed as noise during the binarization. The code stores these data in an Excel file saved in the directory containing the TIFF images.

To calculate the relevant parameters, the MATLAB routine performs a binarization of the original stack by an automatic Otsu thresholding on each plane and corrects the outliers by iterative dilation, fill, and erosion. A mode filtering is also performed to smooth the noise. The code reconstructs the gel height pixel per pixel as the number of stack planes in which each pixel is identified as signal (logical 1 after the binarization) multiplied by the step-to-micron conversion factor of 0.9. Finally, the calculated data is presented to the user with a color-coded heatmap and 3D volume reconstruction of the well. Moreover, the gel profile in the middle of the well is also illustrated, both from raw data and after smoothing with a window of 15 pixels that corresponds to about 20 μm . All the images were also saved in the user-defined directory.

2.5 Preparation of gelatin substrates for cell culture

To make the gelatin layers suitable for cell growth, it is necessary to remove the remaining oil by washing three times with PBS $-/-$. For each washing, 40 μL of PBS $-/-$ was added to each well and removed after 5 minutes to allow phase separation between water and oil. After the third washing, 40 μL of PBS $-/-$

containing 1% of Penicillin/Streptomycin (100x) (SIAL- PEN/STREP) was added and not removed to allow hydrogel rehydration and swelling, favored by overnight rest in the incubator at 37°C. The following morning, the liquid was aspirated and replaced with cell culture media DMEM F-12 (gibco 21041-025). To ensure that all PBS -/- and antibiotic was removed, 80 μ L of DMEM F-12 was added to each well and aspirated twice to dilute the concentration of residual fluid. Finally, 80 μ L of DMEM F-12 was cast again and the plate was placed in the incubator until cell seeding.

3. RESULTS

This section presents the most relevant results and discusses their significance in improving the microfabrication of biologically resemblant platforms for drug screening. First, we test the idea of avoiding the meniscus formation by counterbalancing the surface forces by increasing gravity with a centrifuge and a two-liquid-phase approach. Then, we show how the introduction of an emulsification step improves the coverage of the well area. Lastly, we identify the emulsion formation as the key step to ensure repeatability within the plate and between different plates.

3.1 Two-liquid-phase centrifugation approach

To modify the interfacial surface energy of the hydrogels with a second phase, we first need to determine which liquid to use as the immiscible phase. Comparing the physical and chemical properties of a variety of compounds, we conclude that vegetal oils are our strongest candidates due to a compromise between availability, cost, toxicity, and physical requirements, such as high contact angle. In particular, we select sunflower seed oil as our prime choice because it has one of the highest contact angles between vegetal oils and a relatively low viscosity that makes its use compatible with liquid handling robots.

Then, we experimentally test the combination of centrifugation and surface engineering by oil inclusion. We cast in five wells of a 384-glass bottom well plate 10 μL of food-grade sunflower seed oil and add 1 μL of hydrogel precursor solution in each well, expecting to see a flat interface gel with a height of ~ 100 μm . After casting, we put the plate in the centrifuge precooled at 4°C to ensure a physical setting of the gelatin in a short time. We set the centrifuge at $4000g$, to ensure that surface forces are squared, for 20 minutes, to give the system time to complete the physical setting and start the enzymatic crosslinking before the effect of the centrifuge ends.

After an overnight, the gels are fully crosslinked, and we can perform confocal microscopy to characterize their coverage, height, flatness, and surface roughness. The imaging shows that only one gel of five has the expected profile, while the other four present a large conglomerate of gelatin that is not evenly spread on the bottom of the well, resulting in a doubled height (**Figure 10**).

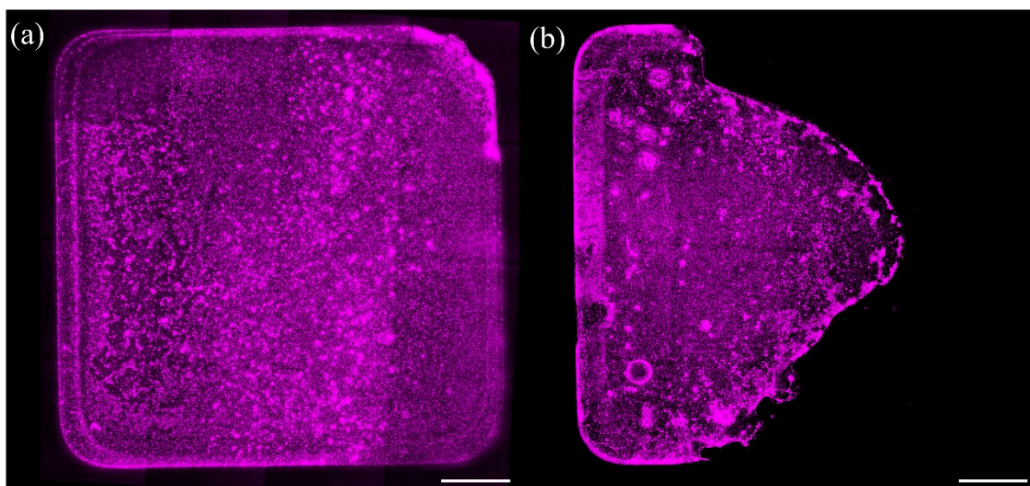


Figure 10 Prove of concept of gel fabrication using centrifugation in a two-liquid phases configuration. Even if it has the potential to result in a flat and spread interface as shown in (a), the yield of this approach is limited as it resulted in 83% of gels in a partial coverage as (b). Scale bars: 500 μm .

While the material of the bottom of the well is glass, the walls of the plate are in polystyrene. Due to the chemical properties of gelatin, it favors adhesion to a polystyrene substrate rather than on glass. Moreover, once the walls are pre-wetted by gelatin, their contact angle lessens and makes further favorable wall adhesion. Lastly, gelatin has strong bounds and tends to stick together, requiring higher forces to break its continuity. If we cast the gelatin drop near a wall, the combination of these factors will cause wall adhesion and incomplete coverage of the bottom. To obtain consistently an evenly spread layer on the bottom of the well, we need to implement some steps to reduce the glass contact angle and to prevent wall prewetting.

3.2 Glass activation, emulsion, and centrifugation approach

To guarantee consistency in forming a spread and flat substrate layer on the bottom of the wells, we need to solve the problems of lower contact angle between polystyrene and gelatin, and wall prewetting and sticking. To favor bottom wetting, we introduce a step of glass activation by adding in each well 10 μ L of 1M NaOH for 1h. This treatment decreases the glass contact angle to values $<25^\circ$ ¹¹ enhancing the spreading of water-based solutions, such as gelatin precursor, as shown in **Figure 11**. To prevent the gelatin from denaturation due to NaOH pH, we rinse the wells three times in abundant DI water and let the plate dry for about

15 minutes before casting. However, gel casting happens within 30 minutes of the activation process to ensure that the lower contact angle is in place.

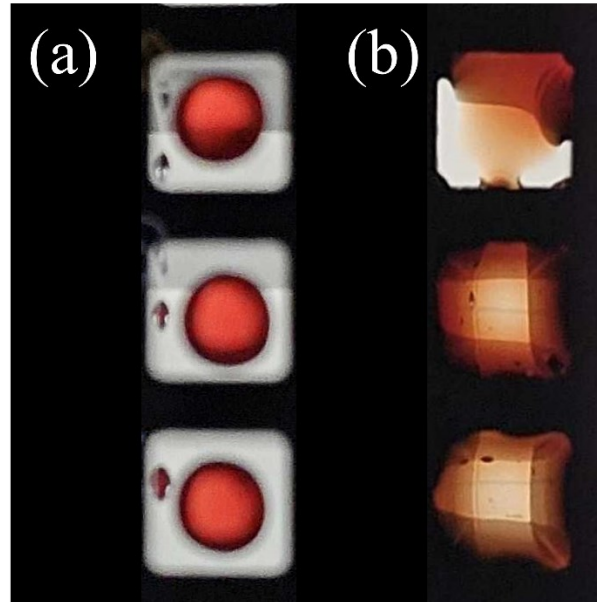


Figure 11 The difference in spreading on untreated (a) and NaOH-treated glass (b). Top view of untreated vs 1-hour NaOH-treated wells after depositing 3 μL of colored water.

To avoid the proximity of the cast gelatin precursor droplet to the walls, preventing the spreading on the whole substrate, we break the continuity of the gelatin by emulsion. We use the same gelatin preparation protocol (10% w/v PG, 2% mTG with a 1:100 ratio of fluorescent beads to characterize the volume by microscopy) but we disperse the gelatin precursor solution in oil by vortexing. We fix the volume of emulsion to cast in each well to 25 μL to ensure that the oil exerts a relevant force on the gelatin layer to obtain a flat interface. Consequently, in an Eppendorf vial, we mix the gelatin precursor in oil with a 4% v/v ratio, which should result in about 1 μL of gelatin in 25 μL of mixture, and vortex the vial for about a minute. Then, we cast 25 μL of emulsion in each NaOH-treated well and put the plate in the centrifuge, starting the preset program (4000g at 4°C for 20

minutes). After an overnight at room temperature to complete the enzymatical cross-linking, we acquire the z-stack of each well and process the images. First, we use Image-J FIJI to remove the autofluorescence noise and improve the signal-to-noise ratio by automatically adjusting the histogram, then we use a self-coded MATLAB routine to quantify the coverage, height, flatness, and surface roughness of the gelatin layer and reconstruct the volume and middle-well profiles.

We observe a high variability of results in the first batch of 12 gels: five are flat layers with a height between 95 and 130 μm and high coverage, five are also flat but with very partial coverage, one is a large agglomerate surrounded by smaller amounts of gelatin, and one has high borders and a flat center. Examples of each kind are shown in **Figure 13**. To collect a significant sample, we repeat the experiment in different batches, observing each time the same range of results described above, with a prevalence of the snowball-like effect. To ensure that the MATLAB routine does not introduce artifacts, we reconstruct the images with the microscope's acquisition package NIS-Element (Nikon), confirming the previous results, as illustrated in **Figure 12**.

To achieve higher repeatability, we formulate hypotheses on problems that can originate the observed results: the variability in coverage suggests that the droplets of gelatin are not evenly distributed in oil, while the snowball-like effect hints that the gelatin setting begins before the plate enters the centrifuge.

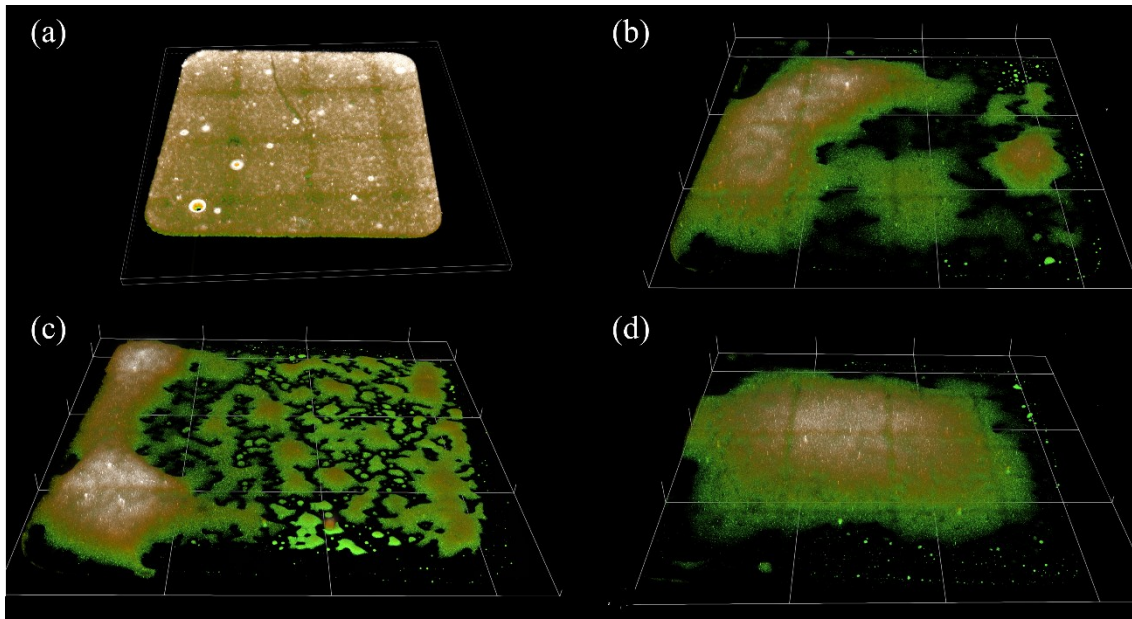


Figure 12 3D reconstruction of gels formed by emulsion and centrifugation of gelatin in oil. To ensure that no artifacts are introduced in the custom MATLAB routine the reconstruction is produced in the microscope's native software (NIS-Element). (a) A flat interface with complete coverage. (b),(c) Different examples of snowball-like effects. (d) A partial coverage layer.

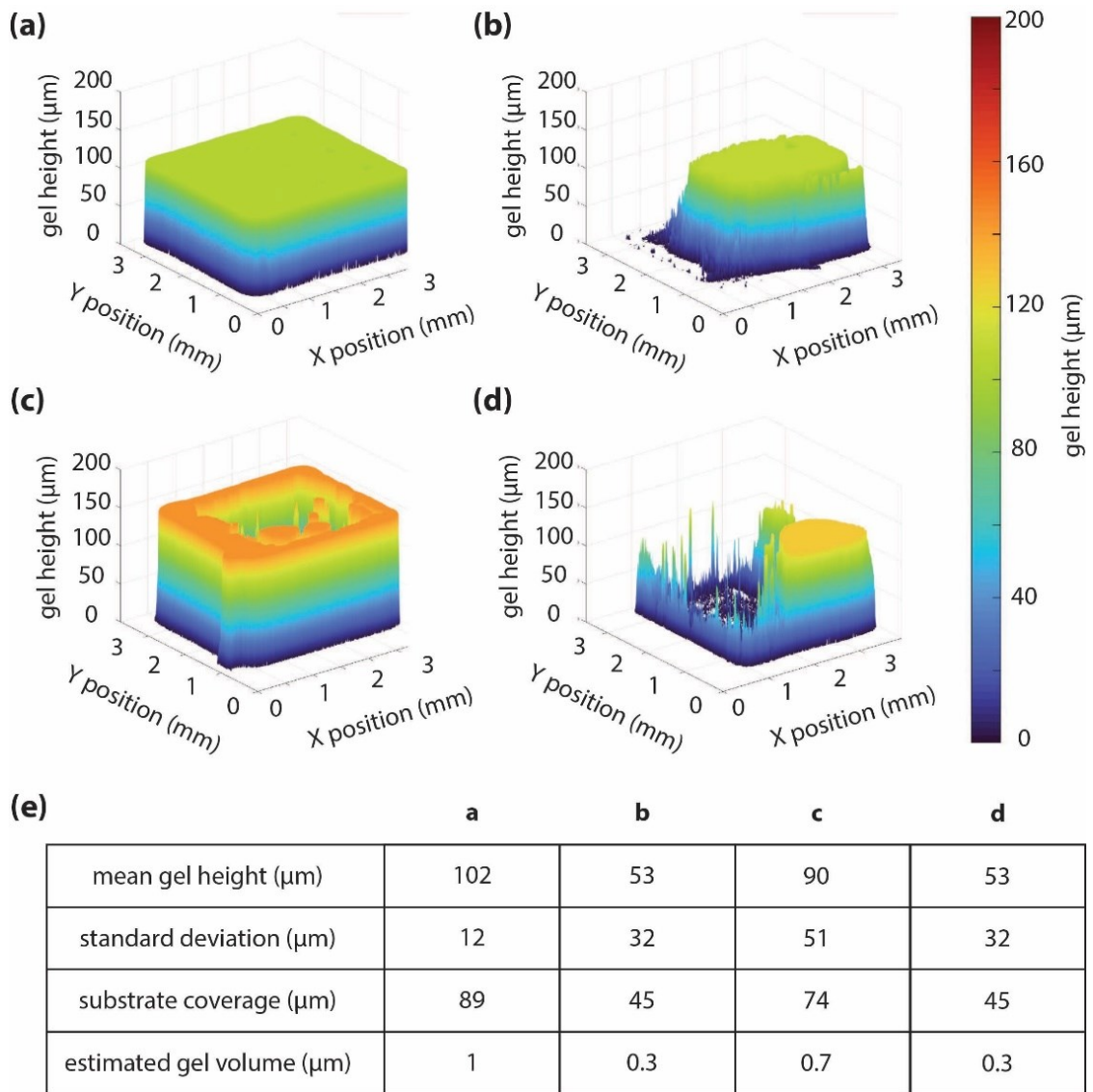


Figure 13 *MATLAB Volume reconstruction of the four types of layers resulting from the combination of emulsion and centrifugation of gelatin in oil. (a) The desired result of a flat and spread interface (b) A flat layer with partial coverage. (c) High edges with an irregular central surface. (d) A large agglomerate of gelatin at the sidewall. (e) Characteristic parameters for each hydrogel.*

3.3 Emulsification is the key step to ensure repeatability

3.3.1 Adding a sonication step ensures emulsion stability

Our experiments demonstrated that by combining emulsification by vortexing with centrifugation we can successfully engineer high-throughput well plates with flat gelatin layers. However, the repeatability of this achievement is scarce, as shown in **Figure 10**, due to the uneven distribution of gelatin droplets in the oil after emulsification by vortexing which causes a fluctuation in the volume of gelatin dispensed in each well.

Moreover, the gelatin precursor composed of 10% PG and 2% mTG tends to set rapidly at ambient temperature, when this happens large precipitates form on the bottom of the mixture container, the volume of gelatin in each well is even more volatile, and snowball-like aggregates cover the well bottom with an uneven layer.

To solve this problem, we modify our precursor solution, halving the concentration of both PG and mTG to delay both the physical setting and the enzymatic crosslinking. A hydrogel precursor composed of 5% w/v PG and 1% w/v mTG is also less viscous and more viable for liquid-handling robots.

To ensure that the gelatin precursor volume in each well is more predictable, we need to obtain droplets with similar diameters evenly distributed in the entire oil

volume, avoiding precipitation, which means a stable emulsion. To form smaller droplets and a stable emulsion, we use a sonicator, which is a machine that induces mechanical waves in water. By immersing the vial containing oil and gelatin precursor in the sonicator after vortexing for 15 seconds, the mechanical waves propagate in the vial, disrupting the precursor solution in smaller droplets distributed in the whole oil volume. After 10 minutes in the sonicator, the mixture has a creamy appearance, characteristic of stable emulsions. To avoid physical setting during this step, the water temperature in the sonicator is around 40°C. Comparing the gelatin droplets diameters and distribution without and with the sonication step, we observe how the stability of the emulsion is the key to obtaining a complete coverage of the well bottom (**Figure 14**).

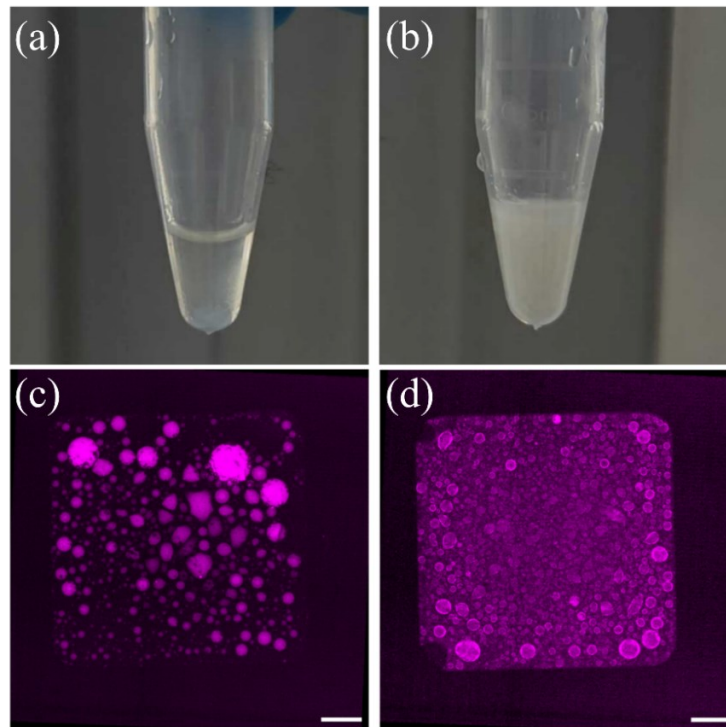


Figure 14 Comparison in emulsion stability between vortexing (left panels) and sonication after vortexing (right panels). (a) and (b) compare the emulsion stability 10 minutes after casting the gels by confronting cross-sectional views of emulsions in Eppendorf vials. In (a) is visible the gelatin precipitate as a blue aggregate on the bottom of the vial, while (b) shows a stable emulsion with the characteristic “creamy” appearance. In (c) and (d) a z-max projection shows the comparison of droplet dimensions and distribution between the emulsification methods in NaOH-treated wells after 20 minutes of static wait (no centrifugation step) in a 4°C fridge. 2 μ L of solution per well, 4X objective, scale bars 500 μ m.

3.3.2 Is centrifugation necessary?

Analyzing the physics underlying the meniscus formation, three different phenomena contribute to the surface curvature: superficial forces dominate gravity, capillarity due to differences in interfacial tension between the solid walls and the fluid (i.e. gelatin and air) at contact, the need for a constant chemical potential, also influenced by surface energy.^{8,9} However, the contribution of each factor cannot be easily quantified.

By introducing a second liquid with a contact angle similar to gelatin, i.e. sunflower seed oil, reducing the energetic advantage in wall wetting by

emulsification and glass treatment, and squaring surface and volume forces by centrifugation, we are tackling all the possible causes. Although, this approach may be unnecessary. As shown in **Figure 14**, a stable emulsion is the key to an even distribution of particles in oil and a spread layer on the bottom of the well. Then, we test the hypothesis that surface energy provides the largest contribution to meniscus formation and consequently the centrifugation step may be superfluous.

To verify this surmise, we produce an emulsion of 5% PG, 1% mTG, and 1:100 fluorescent beads in sunflower seed oil, doubling the ratio of gelatin-in-oil to 8% v/v to avoid the possibility of incomplete coverage due to scarcity of precursor in the sample. Then, we pipette 25 μ L of the mixture from the Eppendorf vial to the NaOH-treated wells and induce the physical setting moving the plate to a 4°C fridge and waiting 20 minutes. Due to the higher density of gelatin precursor we expect sedimentation to happen rapidly. However, if the physical setting process starts inside the droplet they wo not merge, causing a “snowball-like” effect instead of a flat interface. To avoid the effect of physical crosslinking, we favor the transition to enzymatical crosslinking waiting 48h at room temperature before performing imaging. We also test if skipping the 4°C step and letting the gel set for 48h at room temperature eliminates the causes of non-merging droplets and results in flat layers viable for cell growth and high-resolution microscopy.

After 48h, we take the z-stacks of the wells of both batches and repeat the image processing routine: first, we remove the autofluorescence noise and improve the

signal-to-noise ratio by automatically adjusting the histogram in Image-J FIJI, then we pass the pre-processed z-stack to the MATLAB routine we implemented to extract well coverage, mean gel height, flatness and roughness, and infer the effective volume of gel precursor in each well.

Results show in both cases a snowball-like appearance, as illustrated in **Figure 15**, leading to the conclusion that centrifugation is necessary to get a flat interface. Moreover, gels settled at room temperature show great variability in volume (from 0.01 to 0.9 μL) corroborating that the distribution of gelatin droplets in the emulsion is uneven. To obtain flat interfaces of predictable height we need to reintroduce the centrifugation step and find a strategy to even out the precursor distribution in the mixture.

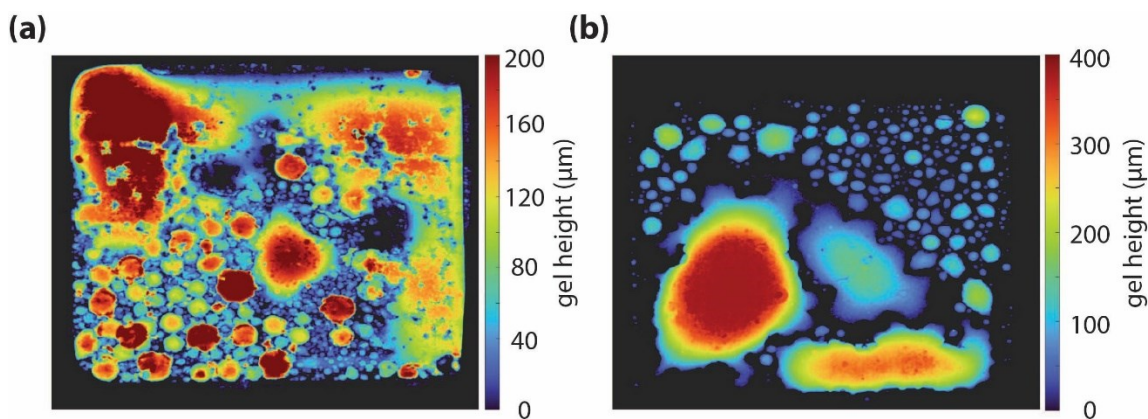


Figure 15 Heatmaps of gel layers formed without centrifugation. (a) gel cooled at 4°C for 20 minutes then left at RT for 48h, colorbar limits 0-200 μm . (b) gel crosslinked at RT for 48h, colorbar limits 0-400 μm .

3.3.3 Adjusting precursor-in-oil ratio for better control of gelatin height

To reach our goal of designing a protocol for flat biomaterial layers in high-throughput well plates viable for high-resolution microscopy and drug screening in industrial settings, we need to confidently predict the final gel height in each well from the volume cast. However, this is possible only if we obtain uniformly spread gelatin droplets in the entire oil volume. During our previous experiments, we failed to produce same-height gels both using the theoretical ratio of 1:25 v/v (see **Figure 12** and **Figure 13**) and doubling this ratio, concluding that the emulsion needs to be sufficiently stable. A water-in-oil emulsion is more stable when the water percentage is higher⁵⁰, although our mixture does not include emulsifiers. Yet, due to its amphiphilic nature, gelatin can be considered an emulsifier itself.

Consequently, we repeat the experiments increasing the volume of gelatin precursor in the mixture. At first, we try doubling again, using a 1:6 ratio that theoretically implies that we cast 2 μL of gelatin precursor in 12.5 μL of emulsion. 2 μL of gelatin should result in gels 200 μm thick, that is on the higher part of the viable range. However, gelatin tends to stick to polystyrene, so we expect a loss due to the material of the pipette tip. Moreover, due to the viscosity of the mixture, the volume we cast does not correspond exactly to the nominal amount. Considering these factors, we expect a nominal volume of 2 μL resulting in layers with a height under 100 μm . Then, we apply the protocol which briefly consists of

NaOH treatment of the glass bottom, 1:1 mixing of mTg and PG, 1:6 mixing of precursor solution in sunflower seed oil, emulsion formation by vortexing and sonication for 10 minutes, casting 12.5 μ L of mixture in each well, transfer the plate in the centrifuge precooled at 4°C, and start the cycle of centrifugation at 4000g for 20 minutes (complete protocol in section **2.2** G-force protocol for thin and flat gels in high-throughput well plates). After the sonication, we notice the presence of aggregates in the creamy mixture.

We perform imaging after 24 hours at room temperature and apply the MATLAB routine to analyze the relevant parameters of the resulting layers, such as well coverage, mean height, and a measure of flatness and roughness of the interface, and to infer a measure of the effective gelatin volume in each well. A graphical representation of the mean height distribution and average deviation from the mean in each well is shown in **Figure 16**. We attribute the significant variation in height to the aspiration of parts of the aggregates, which also determined the presence of lumps and lower surface coverage. However, if we remove the aggregates, we are unsure of the effective volume of gelatin remaining in the emulsion, making the solution not repeatable and consequently incompatible with our goals.

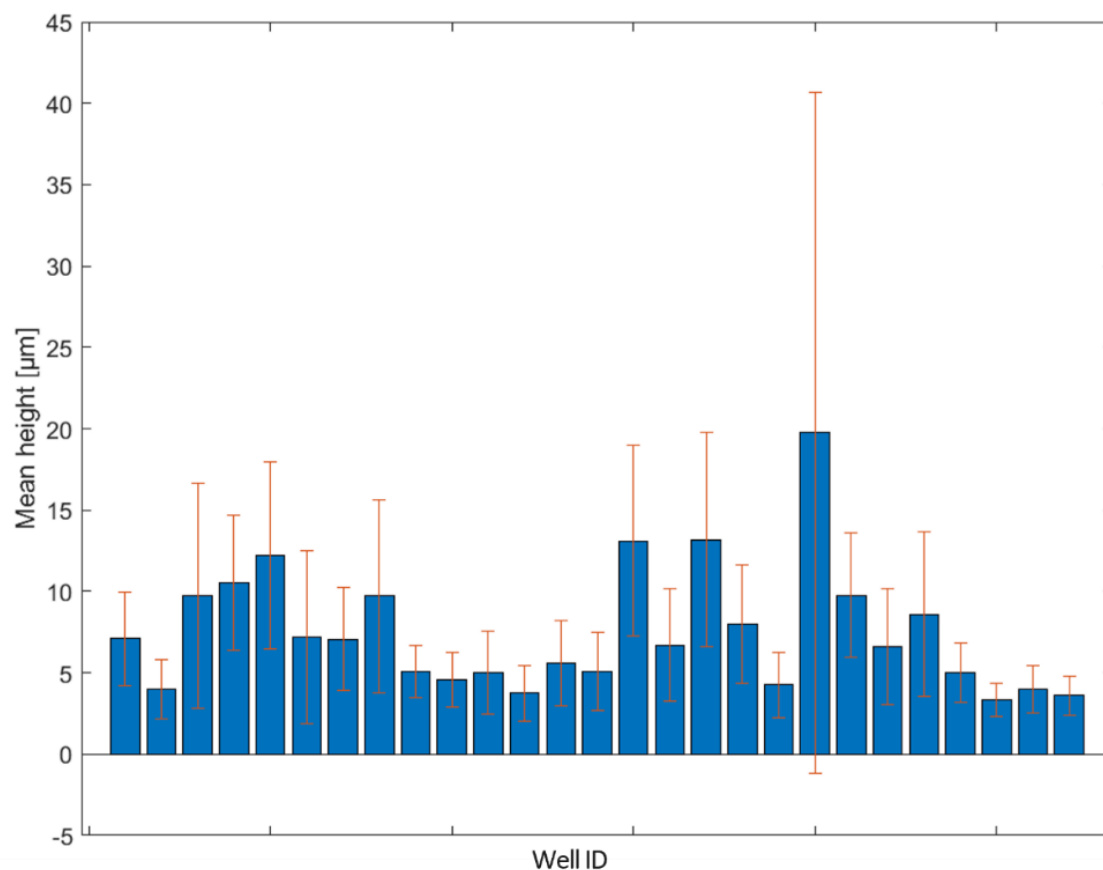


Figure 16 Mean height and average deviation of gelatin layer. Batch cast from a 1:6 precursor-in-oil mixture. Bars indicate the mean height of the hydrogel layer in each well, while lines indicate the average deviation from the mean.

A 1:1 ratio of water-in-oil results in the most stable emulsion⁵⁰, so we test this change in our protocol. We decide to cast 4 μL of the mixture in each well due to the previous considerations on gelatin sticking inside and on the pipette tip, and incomplete volume expulsion. The results from image processing show that the mean height is $60 \mu\text{m} \pm 11 \mu\text{m}$, an 18.3% variation which is incompatible with our goal ($< 10\%$ variation in height between wells). However, the appearance of the mixture is homogeneous, and no lumps are visible, consequently, we conclude that a 1:1 precursor-in-oil ratio forms stable emulsions.

Then, we change the amount of mixture cast in each well to verify if the volume effectively dropped in a well depends on the aspired quantity. Repeating the experiment with a 1:1 ratio but casting 3 μL in each well, we observe an encouraging result: 40 out of 40 samples cast show a coverage $> 80\%$ and a mean height always between 7 and 10 μm , with low average deviation. An example of one gel surface and 3D reconstruction is presented in **Figure 17**. Yet, the mean height of gels is lower than the minimum value that guarantees cell isolation from the rigid substrate. However, the flatness of the interface on the whole well and high repeatability are the primary goals, hence we fix 3 μL as the standard amount, studying how to induce a controlled swelling to match the minimum height requirements.

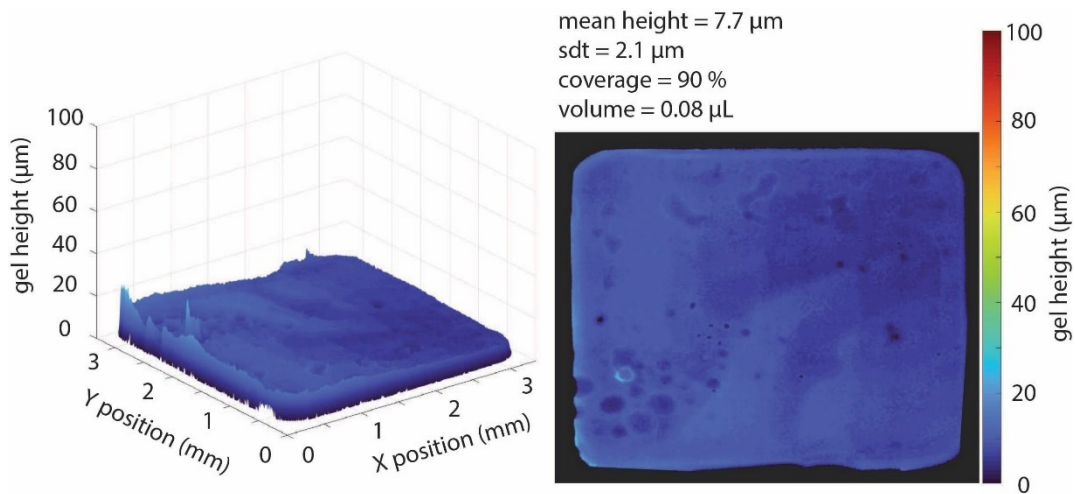


Figure 17 Surface reconstruction and heatmap of an example of 1:1-ratio, 3 μL gels.

To characterize if the designed protocol can match the minimum height requirements for cell growth on a soft substrate, we need to verify the final height after removing the oil and rehydrating the substrate with antibiotics and culture media. First, we perform three washes in PBS $-/-$, to eliminate the remaining

sunflower seed oil from the wells. To avoid ruining the gels by touching them with the pipette tip, we set the aspiration height at 100 μm from the bottom of the plate. To ensure complete remotion of oil, we wait 10 minutes after dispensing PBS -/- to let phase separation occur before reaspiration. After that, we rehydrate and sterilize the gelatin substrate with an overnight incubation of PBS containing 1% Pen Strep at 37°C.

Then, we substitute the liquid with cell culture media DMEM F-12. To warrant the total substitution of PBS, which is incompatible with cell growth, we aspirate the PBS at 100 μm , and we add and then remove DMEM F-12 three times to dilute an eventual remaining volume of PBS. After 48 hours of DMEM F-12 incubation, we perform imaging again and compare the mean height of the hydrogels before and after swelling to verify if the final height is in the goal range, i.e. between 20 and 200 μm . We prepare a new batch of 3 μL , 1:1 gelatin-in-oil ratio gels, consisting of 16 samples. Data show that the mean height after swelling is 23 ± 2 μm , and 14 out of 16 gels have a height greater than 20 μm , as illustrated in **Figure 18**.

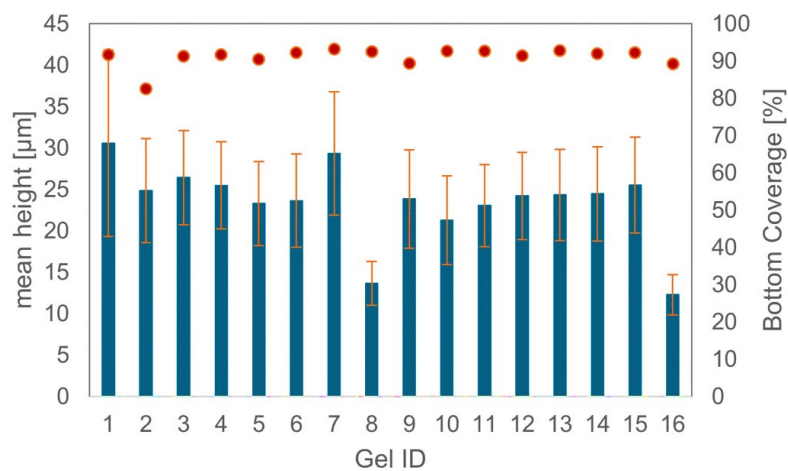


Figure 18 Mean height (blue bar) and percentage of coverage (red dot) of each sample after rehydration

4. CONCLUSIONS

4.1 Discussion of presented results

The main goal of this thesis was to test if we could design a solution to cast full-coverage and flat hydrogel in high-throughput well plates to obtain substrates suitable both for high-resolution microscopy and omics on a large scale. We successfully demonstrated the fabrication of thin and flat gelatin hydrogels with high well coverage in a 384-well plate format. To achieve this result, we combined the emulsification of two liquids with similar interfacial properties, i.e. sunflower seed oil and a gelatin hydrogel precursor, with centrifugation to increase the volume forces and favor phase separation.

To ensure that the protocol is viable on a large scale, we tested how to ensure repeatability in the final height of the layer, verifying the change in the emulsion stability while increasing the gelatin-to-oil ratio. To guarantee a substrate viable for cell growth, we balanced the amount of precursor needed to warrant a flat interface and the minimum requirements to consider the substrate soft for cell culture. We verified that by emulsifying in a 1:1 ratio a PG and mTG precursor solution in sunflower seed oil, we obtained a mixture compatible with liquid handling robots, and we observed that by casting 3 μL in NaOH-treated glass-bottom well plates and centrifuging the plates at 4000g and 4°C for 20 minutes we obtained a flat interface with high repeatability and low variations. We then

showed that swelling can be successfully performed with standard laboratory liquids such as PBS and DMEM F-12. The protocol we developed involved standard and cheap materials and basic laboratory instruments, making it viable for large-scale applications. However, further optimization is needed to propose its integration in R&D pharmaceutical pipelines, as discussed in the following section.

4.2 Open technical challenges and additional insights

The protocol we developed is viable for the functionalization of high-throughput well plates, however, at the moment some technical challenges remain open.

In particular, the 1:1 ratio causes the emulsion to be so stable that sometimes centrifugation cannot phase-separate oil from gelatin, resulting in opaque gels due to the inclusion of oil droplets in the final layer. Due to its amphiphilic nature, gelatin tends to create separation between water and oil, trapping droplets of oil between its chains, in particular when crosslinked with moderate amounts of mTG⁴⁷. When oil is included in gels, it interferes with their optical transparency, lowering the signal and the resolution of microscopy images, which is not compatible with our goal of high-resolution imaging. To demulsify the mixture the easiest path should be decreasing the surfactant, i.e. gelatin, with respect to the amount of oil. Yet, as discussed in section

3.3.3 Adjusting precursor-in-oil ratio for better control of gelatin height the ratio between hydrogel precursor and oil is critical to ensure high repeatability. The first approach to this problem will be sweeping different ratios to verify if an optimum between stability and phase separation exists.

Another possible solution is switching to lighter oil, using for example nonadecane, a non-toxic hydrocarbon with a high contact angle and a density of 0.72 g/mL compared to the 0.92 g/mL density of sunflower seed oil. Since it is

lighter, phase separation should occur easily. Furthermore, the viscosity of the final solution should decrease, making the mixture more compatible with liquid-handling robots. To adopt this solution, however, we should revisit the protocol to work at temperatures above the material melting point, which is 32°C. A more viable solution is to substitute the sonication step with another emulsification technique that results in a less stable system. We consider both stirring⁵⁰ and microfluidization⁴⁸, however, the latter requires specialized instruments, such as a microfluidic chip and a pump, while the former is promising and we plan to test several stirring velocities and mixing temperatures soon. An alternative method is adding a competitive surfactant⁶⁵ which can induce precipitation of the gelatin layer, yet the effects on cell growth should be verified. A different approach could be salting out,⁵⁸ a technique that causes separation between an organic and an aqueous phase in the presence of a large quantity of salts. However, NaCl does not induce the precipitation of gelatin, and the use of other salts or compounds may denature the chains, resulting in substrates not viable for cell growth.

Secondarily, our approach could produce flat hydrogels only in the center of the multiwell plate due to the nature of the Coriolis force profile during centrifugation. In fact, for short rotor radius (14 cm), there is an increasing difference between the direction of the Coriolis force and the normal vector to the surface when moving away from the center of the well plate. As a consequence, gelatin in the lateral wells sets as a flat yet sloped hydrogel, limiting the yield of the proposed solution. Increasing the rotor arm mitigates this problem (**Figure 19**).

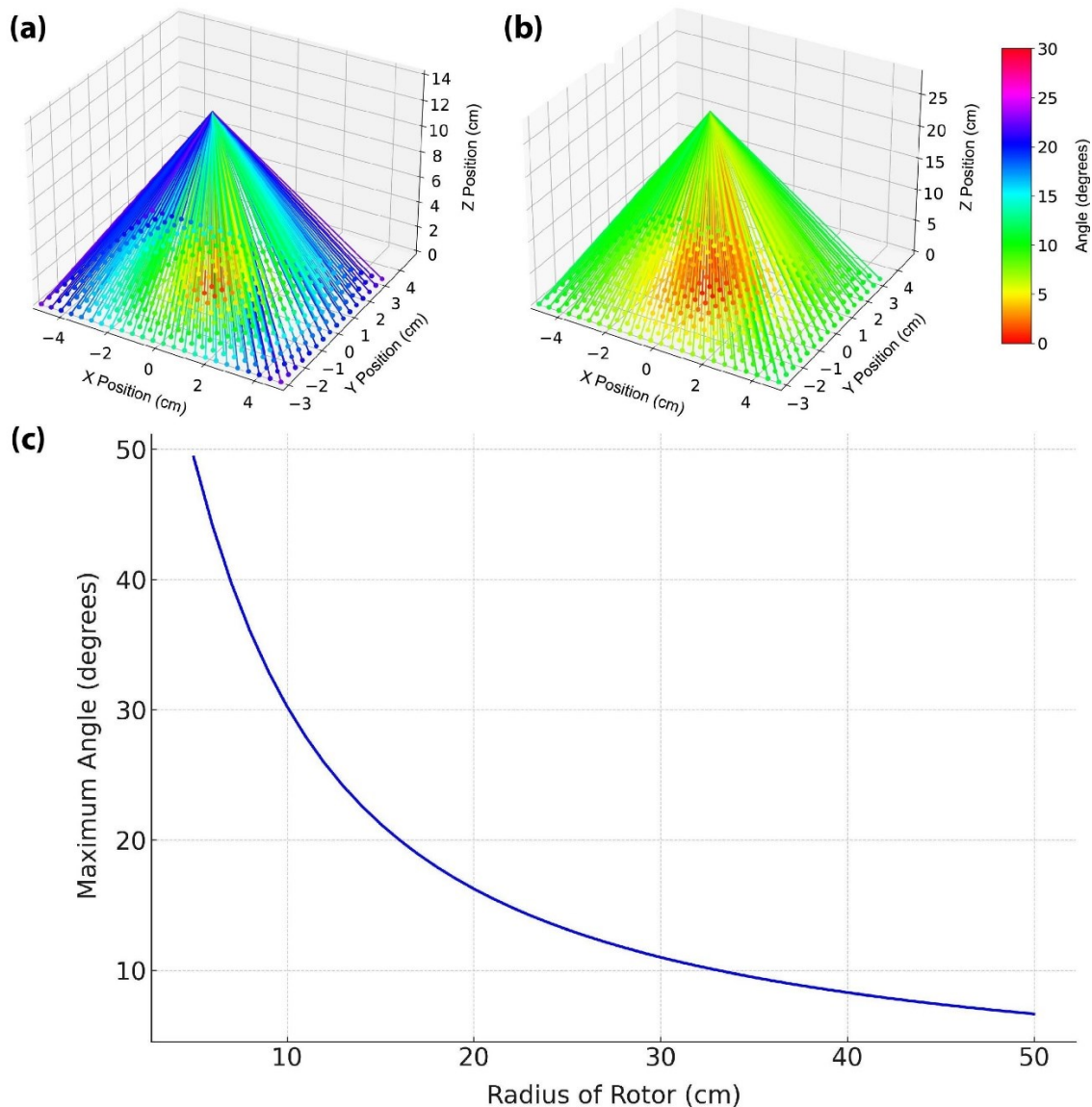


Figure 19 Simulation of slope angles according to plate coordinates and rotor length. (a) Slope angles simulation with arm rotor length fixed at 14 cm, as the centrifuge used to perform the experiments. (b) Slope angles when the arm length is doubled. (c) Curve that describes the maximum slope angle at increasing rotor arm lengths.

In principle, this approach can be adapted to other types of biomaterials, such as hyaluronic acid. To do so, future work should be devoted to studying the emulsification of oil and water phases with other materials than gelatin and setting conditions during centrifugation.

4.3 Outlook

In this study, we designed a pipeline to obtain flat substrate interfaces in 384-well plates, minimizing the number of steps and the complexity of the procedure. Our results show that we can cast gels with a flat profile and a height of $8 \pm 2 \mu\text{m}$ with a pipeline that takes around 2 hours and is highly repeatable. The gels are ready for cell seeding on a layer that isolates cells from the rigid substrate in just 24 hours after production.

As the rising of a meniscus is due to the interfacial properties of solids and fluids, at first, we selected immiscible liquids with similar surface energy properties and demonstrated that the combination of NaOH treatment on glass and emulsification provides layers covering the whole area of the well. Then, we showed that by balancing surface and volume forces using a centrifuge we can obtain a flat interface save for a slope due to angular differences in centrifugal forces direction given by the plate coordinates with respect to the rotor. Lastly, we verified how the stability of the emulsion impacts the predictability of gel height, and we attested that the predictability of final height and the interface flatness are maintained after swelling with various techniques. To extract these results, we implemented a semi-automatic analysis pipeline coding a MATLAB routine for image analysis and volume reconstruction.

Learned the steps needed to obtain a flat interface and developed the tools for analysis, our next goal is the optimization of the protocol, facing open technical

challenges such as the repeatability of phase separation. Then, we plan to test different relevant biomaterials, for example, hyaluronic acid, to verify if our pipeline is a general strategy to overcome the physical phenomena that lead to the meniscus rising in a microfluidic environment. Finally, we intend to demonstrate that the substrates are viable for cell growth and high-resolution microscopy by seeding HaCaT (human keratinocyte) cells and comparing their phenotype with cells cultured on rigid substrates. Further, we want to assess if cells grown on full-coverage hydrogels present different “omics” profiles than cells cultured on traditional stiff platforms, which would confirm that biomaterial flat layers can make a difference in the early stages of preclinical drug screening. This work will be accomplished as part of my Ph.D. in “Design, Modeling, and Simulation in Engineering” in the Synthetic Physiology Laboratory of the University of Pavia.

Bibliography

1. Scannell, J. W., Blanckley, A., Boldon, H. & Warrington, B. Diagnosing the decline in pharmaceutical R&D efficiency. *Nat. Rev. Drug Discov.* **11**, 191–200 (2012).
2. Harrer, S., Shah, P., Antony, B. & Hu, J. Artificial Intelligence for Clinical Trial Design. *Trends Pharmacol. Sci.* **40**, 577–591 (2019).
3. Esch, E. W., Bahinski, A. & Huh, D. Organs-on-chips at the frontiers of drug discovery. *Nat. Rev. Drug Discov.* **14**, 248–260 (2015).
4. Kapałczyńska, M. *et al.* 2D and 3D cell cultures – a comparison of different types of cancer cell cultures. *Arch. Med. Sci. AMS* **14**, 910–919 (2018).
5. McCain, M. L., Agarwal, A., Nesmith, H. W., Nesmith, A. P. & Parker, K. K. Micromolded gelatin hydrogels for extended culture of engineered cardiac tissues. *Biomaterials* **35**, 5462–5471 (2014).
6. Yeh, J. *et al.* Micromolding of shape-controlled, harvestable cell-laden hydrogels. *Biomaterials* **27**, 5391–5398 (2006).
7. Micropatterning Alginate Substrates for In Vitro Cardiovascular Muscle on a Chip - Agarwal - 2013 - Advanced Functional Materials - Wiley Online Library. <https://onlinelibrary.wiley.com/doi/10.1002/adfm.201203319>.
8. Boucher, E. A. Capillary phenomena: Properties of systems with fluid/fluid interfaces. *Rep. Prog. Phys.* **43**, 497–546 (1980).

9. Henriksson, U. & Eriksson, J. C. Thermodynamics of Capillary Rise: Why Is the Meniscus Curved? *J. Chem. Educ.* **81**, 150 (2004).
10. Buxboim, A., Rajagopal, K., Brown, A. E. X. & Discher, D. E. How deeply cells feel: methods for thin gels. *J. Phys. Condens. Matter Inst. Phys. J.* **22**, 194116 (2010).
11. Cras, J. J., Rowe-Taitt, C. A., Nivens, D. A. & Ligler, F. S. Comparison of chemical cleaning methods of glass in preparation for silanization. *Biosens. Bioelectron.* **14**, 683–688 (1999).
12. Commissioner, O. of the. The Drug Development Process. *FDA* <https://www.fda.gov/patients/learn-about-drug-and-device-approvals/drug-development-process> (2020).
13. Blay, V., Tolani, B., Ho, S. P. & Arkin, M. R. High-Throughput Screening: today's biochemical and cell-based approaches. *Drug Discov. Today* **25**, 1807–1821 (2020).
14. Macarron, R. *et al.* Impact of high-throughput screening in biomedical research. *Nat. Rev. Drug Discov.* **10**, 188–195 (2011).
15. Stossi, F. *et al.* High throughput microscopy and single cell phenotypic image-based analysis in toxicology and drug discovery. *Biochem. Pharmacol.* **216**, 115770 (2023).

16. Zemanová, L., Schenk, A., Valler, M. J., Nienhaus, G. U. & Heilker, R. Confocal optics microscopy for biochemical and cellular high-throughput screening. *Drug Discov. Today* **8**, 1085–1093 (2003).
17. Starkuviene, V. & Pepperkok, R. The potential of high-content high-throughput microscopy in drug discovery. *Br. J. Pharmacol.* **152**, 62–71 (2007).
18. Tan, R. K., Liu, Y. & Xie, L. Reinforcement learning for systems pharmacology-oriented and personalized drug design. *Expert Opin. Drug Discov.* **17**, 849–863 (2022).
19. Vincent, F. *et al.* Phenotypic drug discovery: recent successes, lessons learned and new directions. *Nat. Rev. Drug Discov.* **21**, 899–914 (2022).
20. Jaroch, K., Jaroch, A. & Bojko, B. Cell cultures in drug discovery and development: The need of reliable *in vitro-in vivo* extrapolation for pharmacodynamics and pharmacokinetics assessment. *J. Pharm. Biomed. Anal.* **147**, 297–312 (2018).
21. Nawy, T. Single-cell sequencing. *Nat. Methods* **11**, 18–18 (2014).
22. Larsson, L., Frisén, J. & Lundeberg, J. Spatially resolved transcriptomics adds a new dimension to genomics. *Nat. Methods* **18**, 15–18 (2021).
23. Liu, X. *et al.* Spatial multi-omics: deciphering technological landscape of integration of multi-omics and its applications. *J. Hematol. Oncol. J Hematol Oncol* **17**, 72 (2024).

24. High Content Screening - The University of Nottingham.
<https://www.nottingham.ac.uk/life-sciences/facilities/slim/cell-signalling-imaging/high-content-screening/>.
25. Bedia, C. Chapter Two - Experimental Approaches in Omic Sciences. in *Comprehensive Analytical Chemistry* (eds. Jaumot, J., Bedia, C. & Tauler, R.) vol. 82 13–36 (Elsevier, 2018).
26. Joseph, J. S. *et al.* Two-Dimensional (2D) and Three-Dimensional (3D) Cell Culturing in Drug Discovery. in *Cell Culture* (IntechOpen, 2018). doi:10.5772/intechopen.81552.
27. Astashkina, A., Mann, B. & Grainger, D. W. A critical evaluation of in vitro cell culture models for high-throughput drug screening and toxicity. *Pharmacol. Ther.* **134**, 82–106 (2012).
28. Carvalho, V. *et al.* The integration of spheroids and organoids into organ-on-a-chip platforms for tumour research: A review. *Bioprinting* **27**, e00224 (2022).
29. Organotypic and Microphysiological Human Tissue Models for Drug Discovery and Development—Current State-of-the-Art and Future Perspectives | Pharmacological Reviews.
<https://pharmrev.aspetjournals.org/content/74/1/141>.
30. Wang, Y. & Jeon, H. 3D cell cultures toward quantitative high-throughput drug screening. *Trends Pharmacol. Sci.* **43**, 569–581 (2022).

31. Fang, Y. & Eglen, R. M. Three-Dimensional Cell Cultures in Drug Discovery and Development. *SLAS Discov.* **22**, 456–472 (2017).
32. Poenick, S. *et al.* Comparative label-free monitoring of immunotoxin efficacy in 2D and 3D mamma carcinoma in vitro models by impedance spectroscopy. *Biosens. Bioelectron.* **53**, 370–376 (2014).
33. Habanjar, O., Diab-Assaf, M., Caldefie-Chezet, F. & Delort, L. 3D Cell Culture Systems: Tumor Application, Advantages, and Disadvantages. *Int. J. Mol. Sci.* **22**, 12200 (2021).
34. Langhans, S. A. Three-Dimensional in Vitro Cell Culture Models in Drug Discovery and Drug Repositioning. *Front. Pharmacol.* **9**, 6 (2018).
35. How to exploit the features of microfluidics technology. *Lab. Chip* **8**, 20–22 (2008).
36. Berry, J. D., Neeson, M. J., Dagastine, R. R., Chan, D. Y. C. & Tabor, R. F. Measurement of surface and interfacial tension using pendant drop tensiometry. *J. Colloid Interface Sci.* **454**, 226–237 (2015).
37. Lee, B.-B., Ravindra, P. & Chan, E.-S. A Critical Review: Surface and Interfacial Tension Measurement by the Drop Weight Method. *Chem. Eng. Commun.* **195**, 889–924 (2008).
38. Harkins, W. D. & Jordan, H. F. A METHOD FOR THE DETERMINATION OF SURFACE AND INTERFACIAL TENSION FROM THE MAXIMUM PULL ON A RING. *J. Am. Chem. Soc.* **52**, 1751–1772 (1930).

39. Alam, A. U., Howlader, M. M. R. & Deen, M. J. The effects of oxygen plasma and humidity on surface roughness, water contact angle and hardness of silicon, silicon dioxide and glass. *J. Micromechanics Microengineering* **24**, 035010 (2014).
40. Eske, L. D. & Galipeau, D. W. Characterization of SiO₂ surface treatments using AFM, contact angles and a novel dewpoint technique. *Colloids Surf. Physicochem. Eng. Asp.* **154**, 33–51 (1999).
41. Hydrophobic recovery of plasma treated and activated surfaces. *relyon plasma Oberflächenbehandlung* <https://www.relyon-plasma.com/glossary/hydrophobic-recovery/?lang=en>.
42. Enhancing Biocompatibility without Compromising Material Properties: An Optimised NaOH Treatment for Electrospun Polycaprolactone Fibres - Bosworth - 2019 - Journal of Nanomaterials - Wiley Online Library. <https://onlinelibrary.wiley.com/doi/10.1155/2019/4605092>.
43. Evaluation of surface preparation methods for glass - Mellott - 2001 - Surface and Interface Analysis - Wiley Online Library. <https://analyticalsciencejournals.onlinelibrary.wiley.com/doi/10.1002/sia.971>.
44. Goodarzi, F. & Zendehboudi, S. A Comprehensive Review on Emulsions and Emulsion Stability in Chemical and Energy Industries. *Can. J. Chem. Eng.* **97**, 281–309 (2019).

45. Schubert, H. & Armbruster, H. Principles of formation and stability of emulsions. *Int. Chem. Eng.* **32**, 14–28 (1992).
46. Karim, A. A. & Bhat, R. Fish gelatin: properties, challenges, and prospects as an alternative to mammalian gelatins. *Food Hydrocoll.* **23**, 563–576 (2009).
47. Dai, H. *et al.* Designing gelatin microgels by moderate transglutaminase crosslinking: Improvement in interface properties. *Food Hydrocoll.* **149**, 109572 (2024).
48. Jafari, S. M., He, Y. & Bhandari, B. Production of sub-micron emulsions by ultrasound and microfluidization techniques. *J. Food Eng.* **82**, 478–488 (2007).
49. Silva, K. C. G. & Sato, A. C. K. Sonication technique to produce emulsions: The impact of ultrasonic power and gelatin concentration. *Ultrason. Sonochem.* **52**, 286–293 (2019).
50. Chen, G. & Tao, D. An experimental study of stability of oil–water emulsion. *Fuel Process. Technol.* **86**, 499–508 (2005).
51. Starobinets, S., Yakhot, V. & Esterman, L. Critical dynamics of a binary fluid mixture in a centrifugal field. *Phys. Rev. A* **20**, 2582–2589 (1979).
52. Sousa, A. M., Pereira, M. J. & Matos, H. A. Oil-in-water and water-in-oil emulsions formation and demulsification. *J. Pet. Sci. Eng.* **210**, 110041 (2022).
53. Cambiella, A., Benito, J. M., Pazos, C. & Coca, J. Centrifugal Separation Efficiency in the Treatment of Waste Emulsified Oils. *Chem. Eng. Res. Des.* **84**, 69–76 (2006).

54. Peng, L. *et al.* Preparation and characterization of gelatin films by transglutaminase cross-linking combined with ethanol precipitation or Hofmeister effect. *Food Hydrocoll.* **113**, 106421 (2021).
55. Yoshikawa, H., Hirano, A., Arakawa, T. & Shiraki, K. Mechanistic insights into protein precipitation by alcohol. *Int. J. Biol. Macromol.* **50**, 865–871 (2012).
56. Peng, L. *et al.* Effect of different dehydration methods on the properties of gelatin films. *Food Chem.* **374**, 131814 (2022).
57. Hofmeister, F. Zur Lehre von der Wirkung der Salze. *Arch. Für Exp. Pathol. Pharmakol.* **24**, 247–260 (1888).
58. General Principles and Strategies for Salting-Out Informed by the Hofmeister Series | Organic Process Research & Development. <https://pubs.acs.org/doi/10.1021/acs.oprd.7b00197>.
59. Yang, M.-R. *et al.* Hofmeister effect-based soaking strategy for gelatin hydrogels with adjustable gelation temperature, mechanical properties, and ionic conductivity. *Biomater. Adv.* **152**, 213504 (2023).
60. Huang, B. *et al.* Study on Demulsification-Flocculation Mechanism of Oil-Water Emulsion in Produced Water from Alkali/Surfactant/Polymer Flooding. *Polymers* **11**, 395 (2019).

61. Duconseille, A., Astruc, T., Quintana, N., Meersman, F. & Sante-Lhoutellier, V. Gelatin structure and composition linked to hard capsule dissolution: A review. *Food Hydrocoll.* **43**, 360–376 (2015).
62. Liu, Y. *et al.* Tunable physical and mechanical properties of gelatin hydrogel after transglutaminase crosslinking on two gelatin types. *Int. J. Biol. Macromol.* **162**, 405–413 (2020).
63. Zeeb, B., McClements, D. J. & Weiss, J. Enzyme-Based Strategies for Structuring Foods for Improved Functionality. *Annu. Rev. Food Sci. Technol.* **8**, 21–34 (2017).
64. Bertoni, F., Barbani, N., Giusti, P. & Ciardelli, G. Transglutaminase Reactivity with Gelatine: Perspective Applications in Tissue Engineering. *Biotechnol. Lett.* **28**, 697–702 (2006).
65. Zhang, T. *et al.* Gelatins as emulsifiers for oil-in-water emulsions: Extraction, chemical composition, molecular structure, and molecular modification. *Trends Food Sci. Technol.* **106**, 113–131 (2020).

Table of figures

Figure 1 Schematic idea of the work. (a) is a schematic of the profile of an interface with a meniscus. (b) is a schematic of the flattening due to the increase in gravity. (c) is a schematic of the profile when a second liquid phase and an increase in gravity are combined as in G-force. 11

Figure 2 Description of drug development pipeline phases, times, and costs. Reproduced from²..... 14

Figure 3 Schematics of main high-throughput screening methods. (a) Schematics of microscopy screening pipeline. Reproduced from²⁴. (b) Description of the targets of “omics” assays. Reproduced from²⁵. (c) 3D rendering of HaCaT cells (human keratinocytes, in white) seeded on gelatin hydrogel with fluorescent beads (in magenta). Reproduced from previous SPL work. (d) Schematics representation of (c) displaying the mixed cell populations, which is a problem for omics assays. 17

Figure 4 Existing cell culture platforms. From left to right the microenvironment becomes more biomimetic, but also more expensive. Figure reproduced from³⁴. 18

Figure 5 Schematics of the contact angle at a two-fluid interface with a solid well. Bottom liquid (pink) represents the biomaterial precursor, with on top the immiscible liquid (yellow) added as the second phase. At the interface between the two and the solid interface the contact angle is highlighted. The interface between

these two liquids is the surface on which the cells will grow once the biomaterial will harden and the second liquid will be removed.....21

Figure 6 Changes in contact angle before and after surface treatment. (a) Schematics of contact angle changes after plasma treatment. Adapted from ⁴². (b) Changes in contact angle after chemical NaOH treatment: untreated substrate, 0.1M treated substrate, 1M treated substrate. Adapted from ⁴³.....23

Figure 7 Different kinds of emulsions of water (blue) and oil (yellow) in a well. (a) water-in-oil, (b) oil-in-water, (c) oil-in-water-in-oil, (d) water-in-oil-in-water.25

Figure 8 Mechanisms of emulsion separation. Creaming happens when the lighter phase rises to the surface, while sedimentation occurs when the denser phase precipitates at the bottom. Flocculation occurs when the droplets form a larger cluster without merging, while coalescence happens when droplets aggregate by merging.26

Figure 9 Phase separation methods. (a) Schematics of centrifugation process. Due to the increase in gravity (i.e centrifugal force) the denser liquid (in yellow), is subjected to higher force during centrifugation and precipitate at the bottom of the well. (b) Schematics of salting out process due to increase in ion concentration. Reproduced from⁵⁸. (c) Schematics of chemical demulsification. When a demulsifier (yellow dot) is added to the emulsion it competes with the surfactant at the drop interface. Due to its specific properties, the repulsion between drops

lessens and coalescence occurs, the drops merge and become denser allowing phase separation. Reproduced from⁶⁰.....30

Figure 10 Prove of concept of gel fabrication using centrifugation in a two-liquid phases configuration. Even if it has the potential to result in a flat and spread interface as shown in (a), the yield of this approach is limited as it resulted in 83% of gels in a partial coverage as (b). Scale bars: 500 μm41

Figure 11 The difference in spreading on untreated (a) and NaOH-treated glass (b). Top view of untreated vs 1-hour NaOH-treated wells after depositing 3 μL of colored water.43

Figure 12 3D reconstruction of gels formed by emulsion and centrifugation of gelatin in oil. To ensure that no artifacts are introduced in the custom MATLAB routine the reconstruction is produced in the microscope's native software (NIS-Element).....45

Figure 13 MATLAB Volume reconstruction of the four types of layers resulting from the combination of emulsion and centrifugation of gelatin in oil. (a) The desired result of a flat and spread interface (b) A flat layer with partial coverage. (c) High edges with an irregular central surface. (d) A large agglomerate of gelatin at the sidewall. (e) Characteristic parameters for each hydrogel.46

Figure 14 Comparison in emulsion stability between vortexing (left panels) and sonication after vortexing (right panels). (a) and (b) compare the emulsion stability 10 minutes after casting the gels by confronting cross-sectional views of

emulsions in Eppendorf vials. In (a) is visible the gelatin precipitate as a blue aggregate on the bottom of the vial, while (b) shows a stable emulsion with the characteristic “creamy” appearance. In (c) and (d) a z-max projection shows the comparison of droplet dimensions and distribution between the emulsification methods in NaOH-treated wells after 20 minutes of static wait (no centrifugation step) in a 4°C fridge. 2 μL of solution per well, 4X objective, scale bars 500 μm.

.....49

Figure 15 Heatmaps of gel layers formed without centrifugation. (a) gel cooled at 4°C for 20 minutes then left at RT for 48h, colorbar limits 0-200 μm. (b) gel crosslinked at RT for 48h, colorbar limits 0-400 μm. 51

Figure 16 Mean height and average deviation of gelatin layer. Batch cast from a 1:6 precursor-in-oil mixture. Bars indicate the mean height of the hydrogel layer in each well, while lines indicate the average deviation from the mean. 54

Figure 17 Surface reconstruction and heatmap of an example of 1:1-ratio, 3 μL gels...... 55

Figure 18 Mean height (blue bar) and percentage of coverage (red dot) of each sample after rehydration 56

Figure 19 Simulation of slope angles according to plate coordinates and rotor length. (a) Slope angles simulation with arm rotor length fixed at 14 cm, as the centrifuge used to perform the experiments. (b) Slope angles when the arm length

is doubled. (c) Curve that describes the maximum slope angle at increasing rotor arm lengths.61

Acknowledgments

First and foremost, I want to sincerely thank the Synthetic Physiology Lab team. Starting from Professor Francesco Pasqualini, thank you for believing in my potential since the first course you taught me and encouraging me to visit the lab and speak with people to see if I could enjoy Science. It turns out that I do, and I can not express my gratitude enough for renewing your trust in me and supporting my decision to apply for a Ph.D. position at SPL, I'm looking forward to starting this new journey under your supervision.

Thank you to my supervisor, Dr. Alessandro Enrico, for showing me that problems are good and fun, for cultivating a positive attitude where I see failure, for challenging me with a continuous flow of ideas, and for taking the time to discuss each result and problem with encouragement and patience. Thank you so much for guiding me in the writing of this thesis and patiently revising, editing, and suggesting the best words to deliver the message, I learned a lot from you about scientific communication.

Thank you to the wet lab team for teaching me how things work, I feel you all are the kindest and most helpful people to learn from, and I have already understood that you are always right. Thanks for dealing with my million questions and inexplicable daily problems. I swear that the confocal microscope just hates me for no reason. Thank you for finding time and ways to have fun together, and for involving me in the inside jokes.

Then, I really want to thank the people who made my studies in Pavia an enjoyable experience, even with the fog and the lack of sunlight and sea. Just in chronological order, “le ragazze della quarta fila”, in particular Val and Giulia, if it was not for you, I do not know if I would have survived the first year. Thanks to Maha and Rebecca for all the time spent on coding projects and then off-campus, the time we spend together fills my heart with happiness (and envy of your fashion style). Thanks to the crazy Master’s group: Ale, Giulia, Ema, Lavi, Marghe, Marti, Reb, Robby, Vassi, and Virna. You saved me from fainting on the very first day, dealt with my pre-exam anxiety, invited me to the best group study session, coped with my origami passion and my trembling hands, and entertained me with your spontaneity and lack of filters. Our Tuesday lunches are invaluable. Since I’ve met you, I laugh more and get unpredictably embarrassed a lot less, even if knowing you I would never have said, and I feel like this is the best description of these two years.

Lastly, there are a lot of people to thank from home. Starting from my parents, who supported me in this journey. Thanks for always believing in me and encouraging me to catch my dreams away from home. Thanks, Mum, for always stocking my fridge with the best food from home, and for being the best luck charm before the exams. Thanks, Dad, for being proud of me even if I chose to be an engineer. To my brother Nicola, thank you for being my role model and inspiration since I was a kid, you have always been my hero. Thank you for checking all my essays, and for being genuinely interested in my Science journey. To my granny, I know today

you are here and proud of me as you have always been. I wo not ever forget to take time to relax.

Thank you to Silvia, teacher, advisor, and friend. Thank you for encouraging me to broaden my horizons, to ask questions, and to try to find answers.

Thanks to Anna, Lollo, and Pie, thank you for growing up with me and always fueling my passion for Science, since the first discussion on the existence of nothing and the (in)famous hole theory.

Thank you to the Falliti group for supporting me even if you do not understand anything I do and why I love it. Thanks for sticking with me even if I went away and always making me feel part of a group.

Last but not least: thanks, Benji. Thanks for us growing up together and working around the physical distance in this relationship. Thank you for taking care of me, for being a safe space to vent, and for coming to see me even if the climate in Pavia kills your mood. Thank you for cheering me up for each achievement and for being proud of me even if you feel that I do unnecessarily complicated things. I'll stop here. There would be another million things to thank you for, but I have another thesis to write in about three years and I ca not just burn all my cards today.